of tyrosine kinase domain are frequently found in infant ALL with *MLL* rearrangements and pediatric ALL with hyperdiploidy. Blood 2004;103:1085–8.

[13] Shimada A, Taki T, Tabuchi K, Tawa A, Horibe K, Tsuchida M, Hanada R, Tsukimoto I, Hayashi Y. *KIT* mutations, and not *FLT3* internal tandem duplication, are strongly associated with a poor prognosis in pediatric acute myeloid leukemia with t(8;21): a study of the Japanese Childhood AML Cooperative Study Group. Blood 2006;107:1806–9.

[14] Schnittger S, Kinkelin U, Schoch C, Heinecke A, Haase D, Haferlach T, Büchner T, Wörmann B, Hiddemann W, Griesinger F. Screening for MLL tandem duplication in 387 unselected patients with AML identify a prognostically unfavorable subset of AML. Leukemia 2000;14:796–804.

[15] Sheng XM, Kawamura M, Ohnishi H, Ida K, Hanada R, Kojima S, Kobayashi M, Bessho F, Yanagisawa M, Hayashi Y. Mutations of the *RAS* genes in childhood acute myeloid leukemia, myelodysplastic syndrome and juvenile chronic myelocytic leukemia. Leuk Res 1997;21:697–701.

[16] Lange BJ, Kobrinsky N, Barnard DR, Arthur DC, Buckley JD, Howells WB, Gold S, Sanders J, Neudorf S, Smith FO, Woods WG. Distinctive demography, biology, and outcome of acute myeloid leukemia and myelodysplastic syndrome in children with Down syndrome: Children's Cancer Group Studies 2861 and 2891. Blood 1998;91:608–15.

[17] Bunin N, Nowell PC, Belasco J, Shah N, Willoughby M, Farber PA, Lange B. Chromosome 7 abnormalities in children with Down syndrome and preleukemia. Cancer Genet Cytogenet 1991;54: 119–26.

[18] Meshinchi S, Stirewalt DL, Alonzo TA, Zhang Q, Sweetser DA, Woods WG, Bernstein ID, Arceci RJ, Radich JP. Activating mutations of RTK/ras signal transduction pathway in pediatric acute myeloid leukemia. Blood 2003;102:1474–9.

[19] Zwaan CM, Meshinchi S, Radich JP, Veerman AJ, Huismans DR, Munske L, Podleschny M, Hahlen K, Pieters R, Zimmermann M, Reinhardt D, Harbott J, Creutzig U, Kaspers GJ, Griesinger F. *FLT3* internal tandem duplication in 234 children with acute myeloid leukemia: prognostic significance and relation to cellular drug resistance. Blood 2003;102:2387–94.

[20] Liang DC, Shih LY, Hung IJ, Yang CP, Chen SH, Jaing TH, Liu HC, Wang LY, Chang WH. *FLT3*–TKD mutation in childhood acute myeloid leukemia. Leukemia 2003;17:883–6.

[21] Shimada A, Taki T, Tabuchi K, Taketani T, Hanada R, Tawa A, Tsuchida M, Horibe K, Tsukimoto I, Hayashi Y. Japanese Childhood AML Cooperative Study Group. Tandem duplications of *MLL* and *FLT3* are correlated with poor prognoses in pediatric acute myeloid leukemia: a study of the Japanese childhood AML Cooperative Study Group (Epub ahead of print. Aug. 30, 2007). Pediatr Blood Cancer 2007.

[22] Yokota S, Kiyoi H, Nakao M, Iwai T, Misawa S, Okuda T, Sonoda Y, Abe T, Kahsima K, Matsuo Y, Naoe T. Internal tandem duplication of the *FLT3* gene is preferentially seen in acute myeloid leukemia and myelodysplastic syndrome among various hematological malignancies: a study on a large series of patients and cell lines. Leukemia 1997;11:1605–9.

[23] Kottaridis PD, Gale RE, Langabeer SE, Frew ME, Bowen DT, Linch DC. Studies of *FLT3* mutations in paired presentation and relapse samples from patients with acute myeloid leukemia: implications for the role of *FLT3* mutations in leukemogenesis, minimal residual disease detection, and possible therapy with FLT3 inhibitors. Blood 2002;100:2393–8.

[24] Abu-Duhier FM, Goodeve AC, Wilson GA, Gari MA, Peake IR, Rees DC, Vandenberghe EA, Winship PR, Reilly JT. *FLT3* internal tandem duplication mutations in adult acute myeloid leukaemia define a high-risk group. Br J Haematol 2000;111:190–5.

[25] Yamamoto Y, Kiyoi H, Nakano Y, Suzuki R, Kodera Y, Miyawaki S, Asou N, Kuriyama K, Yagasaki F, Shimazaki C, Akiyama H, Saito K, Nishimura M, Motoji T, Shinagawa K, Takeshita A, Saito H, Ueda R, Ohno R, Naoe T. Activating mutation of D835 within the activation loop of FLT3 in human hematologic malignancies. Blood 2001;97: 2434–9.

[26] Thiede C, Steudel C, Mohr B, Schaich M, Schakel U, Platzbecker U, Wermke M, Bornhauser M, Ritter M, Neubauer A, Ehninger G, Illmer T. Analysis of FLT3-activating mutations in 979 patients with acute myelogenous leukemia: association with FAB subtypes and identification of subgroups with poor prognosis. Blood 2002;99: 4326–35.

[27] Bacher U, Haferlach T, Schoch C, Kern W, Schnittger S. Implications of *NRAS* mutations in AML: a study of 2502 patients. Blood 2006;107:3847–53.

[28] Kiyoi H, Naoe T, Nakano Y, Yokota S, Minami S, Miyawaki S, Asou N, Kuriyama K, Jinnai I, Shimazaki C, Akiyama H, Saito K, Oh H, Motoji T, Omoto E, Saito H, Ohno R, Ueda R. Prognostic implication of *FLT3* and *N-RAS* gene mutations in acute myeloid leukemia. Blood 1999;93:3074–80.

[29] Ravindranath Y, Abella E, Krischer JP, Wiley J, Inoue S, Harris M, Chauvenet A, Alvarado CS, Dubowy R, Ritchey AK, Land V, Steuber CP, Weinstein H. Acute myeloid leukemia (AML) in Down's syndrome is highly responsive to chemotherapy: experience on Pediatric Oncology Group AML Study 8498. Blood 1992;80:2210–4.

[30] Lie SO, Jonmundsson G, Mellander L, Siimes MA, Yssing M, Gustafsson G. A population-based study of 272 children with acute myeloid leukaemia treated on two consecutive protocols with different intensity: best outcome in girls, infants, and children with Down's syndrome. Nordic Society of Paediatric Haematology and Oncology (NOPHO). Br J Haematol 1996;94:82–8.

[31] Creutzig U, Ritter J, Vormoor J, Ludwig WD, Niemeyer C, Reinisch I, Stollmann-Gibbels B, Zimmermann M, Harbott J. Myelodysplasia and acute myelogenous leukemia in Down's syndrome: a report of 40 children of the AML-BFM Study Group. Leukemia 1996;10:1677–86.

[32] Kurosawa H, Tsuboi T, Shimaoka H, Okuya M, Nakajima D, Matsunaga T, Hagisawa S, Sato Y, Sugita K, Eguchi M. Long-term remission in an acute monoblastic leukemia patient with Down syndrome after cord blood transplantation [In Japanese]. Rinsho Ketsueki 2005;46:274–7.

[33] Yamaguchi Y, Fujii H, Kazama H, Iinuma K, Shinomiya N, Aoki T. Acute myeloblastic leukemia associated with trisomy 8 and translocation 8;21 in a child with Down syndrome. Cancer Genet Cytogenet 1997;97:32–4.

Fbxw7 acts as a critical fail-safe against premature loss of hematopoietic stem cells and development of T-ALL

Sahoko Matsuoka, Yuichi Oike, Ichiro Onoyama, Atsushi Iwama, Fumio Arai, Keiyo Takubo, Yoichi Mashimo, Hideyuki Oguro, Eriko Nitta, Keisuke Ito, Kana Miyamoto, Hiroki Yoshiwara, Kentaro Hosokawa, Yuka Nakamura, Yumiko Gomei, Hiroko Iwasaki, Yasuhide Hayashi, Yumi Matsuzaki, Keiko Nakayama, Yasuo Ikeda, Akira Hata, Shigeru Chiba, Keiichi I. Nakayama and Toshio Suda

Genes & Dev. 2008 22: 986-991; originally published online Mar 26, 2008;
Access the most recent version at doi:10.1101/gad.1621808

RESEARCH COMMUNICATION

Fbxw7 acts as a critical fail-safe against premature loss of hematopoietic stem cells and development of T-ALL

Sahoko Matsuoka,[1,2] Yuichi Oike,[1,3,4,13] Ichiro Onoyama,[5] Atsushi Iwama,[6,7] Fumio Arai,[1] Keiyo Takubo,[1] Yoichi Mashimo,[8] Hideyuki Oguro,[7] Eriko Nitta,[1] Keisuke Ito,[1,2] Kana Miyamoto,[1] Hiroki Yoshiwara,[1] Kentaro Hosokawa,[1] Yuka Nakamura,[1] Yumiko Gomei,[1] Hiroko Iwasaki,[1] Yasuhide Hayashi,[9] Yumi Matsuzaki,[10] Keiko Nakayama,[11] Yasuo Ikeda,[2] Akira Hata,[7] Shigeru Chiba,[12] Keiichi I. Nakayama,[5] and Toshio Suda[1,6,14]

[1]Department of Cell Differentiation, The Sakaguchi Laboratory, School of Medicine, Keio University, Tokyo 160-8582, Japan; [2]Department of Internal Medicine, School of Medicine, Keio University, Tokyo 160-8582, Japan; [3]PRESTO, Japan Science Technology Agency (JST), Saitama 322-0012, Japan; [4]Department of Molecular Genetics, Graduate School of Medical Sciences, Kumamoto University, Kumamoto 860-8556, Japan; [5]Department of Molecular and Cellular Biology, Medical Institute of Bioregulation, Kyushu University, Fukuoka 812-8582, Japan; [6]CREST, Japan Science Technology Agency (JST), Saitama 322-0012, Japan; [7]Department of Cellular and Molecular Medicine, Chiba University, Chiba 260-8670, Japan; [8]Department of Public Health, Graduate School of Medicine, Chiba University, Chiba 260-8670, Japan; [9]Department of Hematology/Oncology, Gunma Children's Medical Center, Gunma 377-8577, Japan; [10]Department of Physiology, School of Medicine, Keio University, Tokyo 160-8582, Japan; [11]Department of Developmental Biology, Graduate School of Medicine, Tohoku University, Sendai 980-8575, Japan; [12]Department of Cell Therapy and Transplantation Medicine, University of Tokyo Hospital, Tokyo 113-8655, Japan

Common molecular machineries between hematopoietic stem cell (HSC) maintenance and leukemia prevention have been highlighted. The tumor suppressor Fbxw7 (F-box and WD-40 domain protein 7), a subunit of an SCF-type ubiquitin ligase complex, induces the degradation of positive regulators of the cell cycle. We demonstrate that inactivation of *Fbxw7* in hematopoietic cells causes premature depletion of HSCs due to active cell cycling and p53-dependent apoptosis. Interestingly, *Fbxw7* deletion also confers a selective advantage to cells with suppressed p53 function, eventually leading to development of T-cell acute lymphoblastic leukemia (T-ALL). Thus, Fbxw7 functions as a fail-safe mechanism against both premature HSC loss and leukemogenesis.

Supplemental material is available at http://www.genesdev.org.

Received October 1, 2007; revised version accepted February 22, 2008.

[*Keywords*: Fbxw7; c-Myc; Notch1; p53; hematopoiesis; T-ALL]

Corresponding authors.
[13]**E-MAIL oike@gpo.kumamoto-u.ac.jp; FAX 81-96-373-5145.**
[14]**E-MAIL sudato@sc.itc.keio.ac.jp; FAX 81-3-5363-3474.**

Article published online ahead of print. Article and publication date are online at http://www.genesdev.org/cgi/doi/10.1101/gad.1621808.

Stem cells in various organ tissues are governed by general genetic programs that maintain their common features, including self-renewal and multipotency. Recent studies have demonstrated that it is crucial for hematopoietic stem cells (HSCs) to be quiescent for protection against oxidative stress and to sustain self-renewal capacity (Ito et al. 2004; Tothova et al. 2007). Most HSCs remain quiescent when located in the stem cell niche (Calvi et al. 2003; Zhang et al. 2003; Arai et al. 2004). Once HSCs are released from the niche, they enter the cell cycle and start to proliferate. Cell cycle kinetics of HSCs are strictly controlled by various systems to sustain blood cell production throughout life (Cheng et al. 2000). These findings indicate that precise regulation of the cell cycle in stem cells is essential to maintain stem cell phenotype. The ubiquitin–proteasome system plays a critical role in controlling physiologic events—such as cell cycle progression, apoptosis, signal transmission, and repair of DNA damage—through protein degradation (Fuchs 2005; Minella and Clurman 2005; Welchman et al. 2005; Nakayama and Nakayama 2006). Fbxw7 (F-box and WD-40 domain protein 7)—also known as Fbw7, Sel-10, hCdc4, or hAgo—is an SCF ubiquitin ligase component catalyzing ubiquitination of Myc, cyclin E, Notch, and c-Jun, all of which positively regulate the cell cycle. We hypothesized that a protein like Fbxw7 may play a pivotal role in controlling the HSC cell cycle and maintaining normal hematopoiesis. Tetzlaff et al. (2004) and we (Tsunematsu et al. 2004) independently reported that *Fbxw7*-deficient mice die at embryonic day 10.5 and exhibit deficiencies in hematopoietic and vascular development, suggesting that Fbxw7 functions in hematopoiesis. Mutations in *FBXW7* have been detected in certain human malignancies, including T-cell acute lymphoblastic leukemia (T-ALL) (Spruck et al. 2002; Ekholm-Reed et al. 2004; Mao et al. 2004; Maser et al. 2007). Recent reports have highlighted the existence of molecules operating differentially in the self-renewal of both normal tissue stem cells and cancer stem cells (Yilmaz et al. 2006; Zhang et al. 2006). In this study, we addressed this issue by examining the effect of *Fbxw7* deletion on the maintenance of HSCs and leukemogenesis. Here, we demonstrate that inactivation of *Fbxw7* in bone marrow (BM) HSCs leads to premature depletion of normal HSCs due to active cell cycling and promotes T-ALL due to a compromised p53 response. Thus, Fbxw7 acts as a critical fail-safe against premature loss of HSCs and development of T-ALL (Supplemental Fig. S1).

Results and Discussion

We examined *Fbxw7* expression by quantitative RT–PCR in various hematopoietic lineages sorted from adult mouse tissues. *Fbxw7* was expressed abundantly in most of the hematopoietic cells tested, including $Lin^-Sca\text{-}1^+c\text{-}Kit^+$ (LSK) $CD34^-$ HSCs (Supplemental Fig. S2).

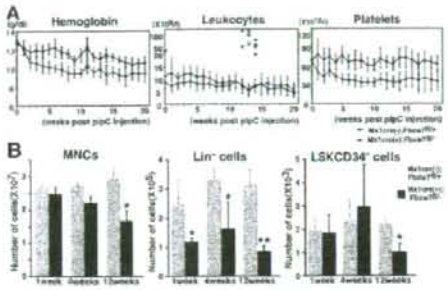

Figure 1. Fbxw7 is essential to maintain the adult hematopoietic pool. (*A*) Peripheral blood cell counts of Fbxw7-deficient (red closed circles, $n = 15$) and control (black closed circles, $n = 15$) mice after pIpC treatment. Results are shown as means ± SD. Red open circles indicate white blood cell counts of mice developing leukemia. (*B*) Absolute numbers of MNCs, Lin⁻ cells, and LSK CD34⁻ HSCs in *Fbxw7*-deficient and control BM at 4, 8, and 12 wk after pIpC treatment. Results are shown as means ± SD from six to eight independent experiments. (*) $P < 0.05$; (**) $P < 0.01$.

To investigate the role of Fbxw7 in adult tissues, we generated *Fbxw7*$^{fl/fl}$ mice in which *Fbxw7* was deleted conditionally in targeted cells (Onoyama et al. 2007). In this study, we created *Mx-1-Cre(+);Fbxw7*$^{fl/-}$ mice by crossing *Mx-1-Cre(+);Fbxw7*$^{+/-}$ mice and *Fbxw7*$^{fl/fl}$ mice in order to investigate the role of Fbxw7 in hematopoietic cells. pIpC was injected into the 8-wk-old *Mx-1-Cre(+);Fbxw7*$^{fl/-}$ mice every other day for 1 wk to induce *Cre* expression and thereby delete *Fbxw7* in their hematopoietic cells. *Mx-1-Cre(−);Fbxw7*$^{fl/+}$ littermates treated with pIpC served as controls. *Mx-1-Cre(−);Fbxw7*$^{fl/-}$ and *Mx-1-Cre(+);Fbxw7*$^{fl/+}$ littermates showed no significant difference from control mice in our analysis (data not shown). We confirmed that *Fbxw7* deletion was induced in BM cells as early as 3 d after pIpC treatment (Supplemental Fig. S3A).

We analyzed peripheral blood cell counts of *Fbxw7*-deficient mice. Levels of hemoglobin and platelets were markedly lower compared with controls immediately after pIpC treatment (Fig. 1A). However, these levels stopped decreasing ~12–16 wk after pIpC treatment. Genomic PCR analysis detected a significant amount of unexcised floxed allele in *Fbxw7*-deficient hematopoietic cells 16 wk after pIpC treatment (Supplemental Fig. S3B). These data suggest that hematopoiesis was compromised in the absence of Fbxw7 after pIpC treatment, whereas the few cells that retained the unexcised *Fbxw7* allele gradually competed out the *Fbxw7*-deficient hematopoietic cells.

The number of the Lin⁻ cells was also reduced immediately in *Fbxw7*-deficient BM after pIpC treatment. In contrast, the number of BM mononuclear cells (MNCs) and LSK CD34⁻ HSCs remained within normal range at the beginning of treatment but was decreased significantly by 12 wk of pIpC treatment (Fig. 1B). The size of the thymus was also reduced significantly in *Fbxw7*-deficient mice (data not shown). To determine whether Fbxw7 is essential for HSC differentiation, we examined the proportion of differentiated cells in *Fbxw7*-deficient BM by flow cytometry. Although a portion of lymphoid cells was decreased slightly, populations of cells sufficient to generate both mature myeloid and lymphoid cells were observed in *Fbxw7*-deficient BM 4 wk after pIpC treatment (Supplemental Fig. S4A). Moreover, in vitro assays revealed that colony-forming capacity was comparable between control and *Fbxw7*-deficient LSK cells (Supplemental Fig. S4B). Morphological analysis of colonies demonstrated the full range of differentiation capacity in *Fbxw7*-deficient LSK cells along the myeloid lineage (data not shown). These data indicate that Fbxw7 is dispensable for multilineage terminal differentiation.

To examine the repopulating capability of *Fbxw7*-deficient HSCs, we transplanted 1500 LSK BM cells from *Fbxw7*-deficient mice or littermate controls 4 wk after pIpC treatment into lethally irradiated recipients using 4×10^5 normal BM mononuclear competitor cells. Although there was no significant difference in the proportion of LSK CD34⁻ HSCs within injected LSK cells, *Fbxw7*-deficient LSK cells showed severely impaired repopulating capacity (Fig. 2A, left). To confirm whether Fbxw7 intrinsically regulates HSC repopulating capability, we transplanted 4×10^5 BM MNCs from either *Mx-1-Cre(+);Fbxw7*$^{fl/-}$ mice before pIpC treatment or littermate controls into lethally irradiated recipients with the same numbers of competitor cells. Two months later, we confirmed that donor cells were reconstituted in recipient BM and then injected the recipient mice with pIpC. Within 1 mo following pIpC treatment, *Fbxw7*-deficient HSCs lost long-term repopulating capability and were eventually competed out by wild-type HSCs (Fig. 2A, right).

It has been reported that most HSCs remain quiescent and that excessive acceleration of the HSC cell cycle

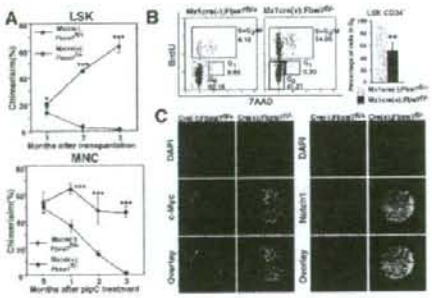

Figure 2. Reconstitution capacity and quiescence are impaired in *Fbxw7*-deficient HSCs. (*A*) Competitive repopulation analysis. (*Left*) Recipient Ly5.1 mice ($n = 6$) were transplanted with 1500 *Fbxw7*-deficient or control LSK cells together with 4×10^5 Ly5.1 × Ly5.2 competitor BM MNCs. Donor-derived chimerism of peripheral white blood cells was analyzed monthly after transplantation. (*Right*) Recipient Ly5.1 mice ($n = 10$) were transplanted with 4×10^5 BM MNCs from *Mx-1-Cre(+);Fbxw7*$^{fl/-}$ mice before pIpC treatment or with controls together with the same number of Ly5.1 × Ly5.2 competitor BM MNCs. pIpC treatment of recipient mice was performed 2 mo after transplantation. Donor-derived chimerism of peripheral white blood cells was then analyzed monthly after pIpC treatment. Results are shown as means ± SD. (*B*) Cell cycle status of LSK CD34⁻ cells of *Fbxw7*-deficient or control mice. BrdU was administered for 3 d to mark cells that entered S phase, and 7-aminoactinomycin D (7-AAD) was administered to detect DNA content. Data shown are representative FACS patterns derived from three independent experiments (*left*) and graphs showing the mean percentage of cells in G_0 (*right*). (*C*) LSK cells isolated from *Fbxw7*-deficient or control mice were stained with DAPI (blue) and anti-c-Myc antibody or anti-Notch1 antibody (green).

leads to their exhaustion (Hock et al. 2004; Ito et al. 2004). Since Fbxw7 functions as a master regulator of the cell cycle by regulating protein levels of cell cycle-related molecules, we hypothesized that a dysregulated HSC cell cycle leads to a decrease in HSC number in *Fbxw7*-deficient mice. To address this possibility, we examined the cell cycle status of *Fbxw7*-deficient HSCs using a BrdU assay. The population of *Fbxw7*-deficient LSK CD34$^-$ HSCs in G_0 was decreased significantly compared with controls (Fig. 2B). We also monitored proliferation of single LSK CD34$^-$ HSCs in culture for 7 d. The frequency of cell division seen in *Fbxw7*-deficient HSCs was markedly increased in culture (data not shown). These data suggest that Fbxw7 functions to maintain HSC quiescence. It has been reported that c-Myc, an Fbxw7 substrate, promotes re-entry of quiescent HSCs into the cell cycle by inducing release of HSCs from the stem cell niche, leading to loss of self-renewal activity at the expense of differentiation (Wilson et al. 2004). c-Myc protein significantly accumulated in *Fbxw7*-deficient LSK cells (Fig. 2C), suggesting that c-Myc-induced active cell cycling of *Fbxw7*-deficient HSCs largely accounts for premature loss of HSCs. This hypothesis would be strongly supported by the observation that inactivation of c-Myc rescued the phenotype of hyperproliferation of DP T cells and the occurrence of lymphoma in *Fbxw7*-deficient thymocytes (Onoyama et al. 2007). In addition, Notch1 protein, which also accumulated in *Fbxw7*-deficient LSK cells, might accelerate HSC differentiation (Fig. 2C; Pui et al. 1999). The levels of c-Jun, another Fbxw7 target, in *Fbxw7*-deficient LSK cells were equivalent to those in the control cells, suggesting that c-Jun did not contribute to the hematopoietic abnormalities in *Fbxw7*-deficient mice (Supplemental Fig. S5). To clarify the time course of activation of these target genes, we performed immunocytochemical staining for c-Myc and Notch at 0, 72, and 96 h after a single injection of pIpC (700 µg) (Supplemental Fig. S6). Nuclear accumulation of c-Myc began within 72 h, and reached plateau by 96 h after pIpC treatment. On the other hand, marked accumulation of Notch1 in nuclei occurred within 72 h after pIpC treatment. These observations indicated that ubiquitin–proteasome-dependent degradation of Notch1 and c-Myc was inhibited rapidly after *Fbxw7* deletion by an initial single pIpC treatment. Interestingly, the accumulation of Notch1 reached plateau slightly earlier than that of c-Myc. It has been found recently that Notch1 directly regulates c-Myc transcription in normal and leukemic T cells (Weng et al. 2006). These studies suggest that the up-regulation of c-Myc expression in *Fbxw7*-deficient HSCs might be enhanced subsequently by Notch1 at the transcriptional level to some extent, in addition to increased protein stability in the absence of Fbxw7.

About 30% of *Fbxw7*-BM-deficient mice showed extremely severe pancytopenia 12 wk after pIpC treatment (Fig. 3A). These mice showed a marked decrease in the number of BM MNCs, including all lineages of hematopoietic cells. It has been suggested that enhanced c-Myc expression likely activates a p53-dependent checkpoint and induces apoptosis, thereby protecting cells from hyperproliferative oncogenic signals (Zindy et al. 1998). Actually, p53 protein was markedly accumulated in ~80% of *Fbxw7*-deficient LSK cells (Supplemental Fig. S7), while there was no difference in p53 mRNA levels between *Fbxw7*-deficient HSCs and the controls (Supplemental Fig. S8). Instead, Mdm2 expression was markedly down-regulated in *Fbxw7*-deficient HSCs at both the mRNA and protein levels (Supplemental Figs. S7, S8). Since it is believed that Mdm2 suppresses p53 function by promoting protein degradation via its E3 ligase activity, p53 may be up-regulated in *Fbxw7*-deficient HSCs, at least partly, through Mdm2 inactivation, although the mechanism underlying reduced Mdm2 protein levels remains elusive. We therefore hypothesized that the drastic reduction of hematopoietic cell number in these mice was caused not only by the dysregulated cell cycle but also by p53-dependent apoptosis. Indeed, the population of apoptotic cells in BM MNCs and HSCs increased substantially in mice with leukopenia compared with those without leukopenia (Fig. 3B). We next asked whether there is a correlation between apoptosis and p53 expression levels in *Fbxw7*-deficient BM cells. p53 protein levels were up-regulated in BM cells derived from all *Fbxw7*-deficient mice 4 wk after pIpC treatment (Fig. 3C, left). In contrast, p53 protein levels were decreased in BM MNCs of *Fbxw7*-deficient mice that showed no leukopenia at 12 wk after pIpC treatment (Fig. 3C, right). These findings suggest that the variations in white blood cell count data could be attributable to the differential modes of p53-dependent checkpoint responses, which induce apoptosis. This notion was further supported by the absence of abnormal ploidy, which could lead to apoptotic cell death, in *Fbxw7*-deficient BM cells (data not shown). It is well recognized that senescence as well as apoptosis is a tumorigenesis barrier (Collado et al. 2005). However, gene expression of *p16^{Ink4a}* was not increased in *Fbxw7*-deficient HSCs (Supplemental Fig. S8) and senescence-associated (SA)-β-galactosidase activity was not considerably detected in *Fbxw7*-deficient LSK cells (data not shown), indicating that *Fbxw7* deletion did not promote cellular senescence.

Interestingly, more than half of the *Fbxw7*-deficient mice developed T-ALL (20 of 34; 59%) within 16 wk of

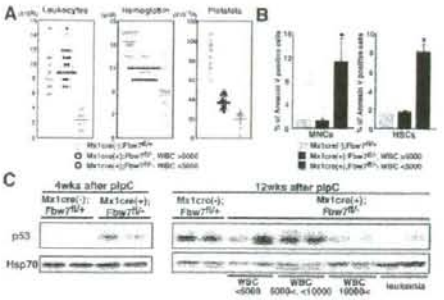

Figure 3. The fate of *Fbxw7*-deficient hematopoietic cells is determined by p53 expression. (*A*) Peripheral blood cell counts of *Fbxw7*-deficient (WBC < 5000, red circle, $n = 24$; WBC > 5000, blue circle, $n = 10$) and control (gray circle, $n = 13$) mice 12 wk after pIpC treatment. Horizontal lines indicate mean values. Closed circles indicate the data for mice that developed leukemia ultimately. (*B*) Percentage of annexin V-positive apoptotic cells in Fbxw7-deficient (WBC < 5000, red bar; WBC > 5000, blue bar) and control (gray bar) BM MNCs (*left*) or LSK CD34$^-$ HSCs (*right*) 12 wk after pIpC treatment. Results are shown as means ± SD from four independent experiments. (*) $P < 0.05$. (*C*) Western blot analysis of p53 in BM MNCs from control and Fbxw7-deficient mice 4 wk (*left*) and 12 wk (*right*) after pIpC treatment. Hsp70 was used as a loading control.

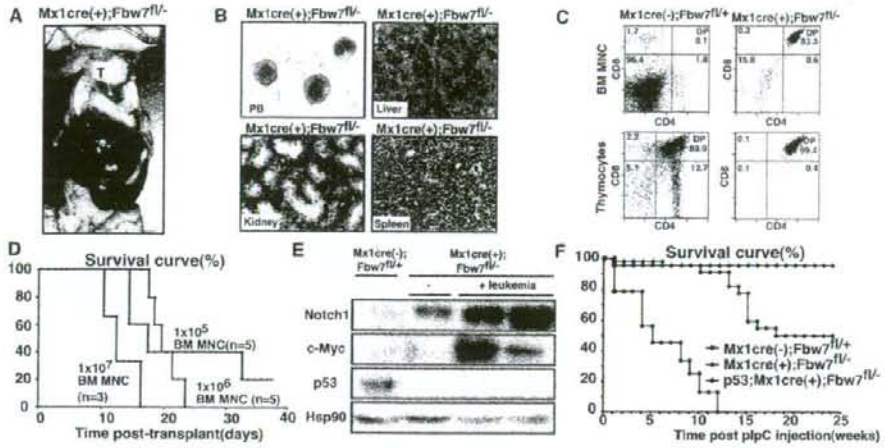

Figure 4. Fbxw7 deficiency in adult hematopoietic cells leads to T-ALL. (*A*) Representative autopsy of leukemic *Fbxw7*-deficient mice. Thymus (T), liver (L), spleen (S), and lymph nodes (arrowheads) were massively swollen. (*B*) Representative histology of peripheral blood (PB), liver, kidney, and spleen from leukemic *Fbxw7*-deficient mice. (*C*) FACS analysis of BM MNCs and thymocytes from leukemic *Fbxw7*-deficient and control mice. Data shown are representative FACS patterns derived from five independent experiments. (*D*) Survival curves for mice injected with graded doses (1×10^5, blue; 1×10^6, red; or 1×10^7 B, green) of leukemic *Fbxw7*-deficient BM MNCs. The average portion of $CD4^+CD8^+$ leukemic blasts in leukemic *Fbxw7*-deficient BM MNCs was 92.4 ± 3.1%. (*E*) Western blot analysis of Notch, c-Myc, and p53 in thymocytes from control, *Fbxw7*-deficient, and leukemic *Fbxw7*-deficient mice. (*F*) Survival curves for *Fbxw7*-deficient (red, $n = 23$), $p53^{-/-}$;*Fbxw7*-deficient (blue, $n = 9$), and control (black, $n = 25$) mice after pIpC treatment.

pIpC treatment (Fig. 4A). In the leukemic mice, lymphoid blasts aggressively invaded BM, liver, spleen, thymus, and kidney (Fig. 4B). Flow cytometry analysis showed that blasts expressed both CD4 and CD8 (Fig. 4C). Furthermore, irradiated mice transplanted with these leukemia cells died of T-ALL within 1 mo (Fig. 4D), indicating *Fbxw7* deletion promoted generation of T-ALL-initiating cells. Most of the *Fbxw7*-deficient mice that did not exhibit leukopenia at 12 wk after pIpC developed T-ALL (20 of 24; 83%) within 16 wk of pIpC treatment, while no *Fbxw7*-deficient mice that exhibited leukopenia led to leukemia (Fig. 3A).

Importantly, leukemic cells of *Fbxw7*-deficient mice displayed significant accumulation of Notch1 and c-Myc proteins (Fig. 4E). Interestingly, the Notch1/c-Myc signaling axis is causally linked to T-ALL development (Weng et al. 2006). These findings suggest that accumulated Notch1 and c-Myc proteins in *Fbxw7*-deficient BM cells caused extrathymic development of T-lineage cells and induced T-ALL. Of note was that p53 protein expression was repressed during leukemogenesis (Fig. 4E). *Fbxw7* deficiency in hematopoietic cells caused only T-cell malignancy, presumably due to Notch1 accumulation, which induces T-lineage commitment in immature cells (Look 2004; Grabher et al. 2006). Constitutive Notch1 activation in hematopoietic stem or progenitor cells blocks B-cell differentiation and expands extrathymic DP T cells in BM, eventually leading to development of T-ALL in BM (Pui et al. 1999). In human T-ALL, Notch1 is the most commonly mutated gene (Weng et al. 2004). While *Fbxw7*-deficient mice did not show a block in B-cell differentiation (data not shown), they did exhibit extrathymic development of DP T cells and T-ALL. In this regard, T-ALL development can be attributed largely to an activated Notch pathway in *Fbxw7*-deficient mice. In contrast, deletion of *Fbxw7* in the thymus of *Lck-cre(+);Fbxw7*$^{fl/fl}$ mice (*Fbxw7*-thymus-deficient mice) promotes development of $CD4^+CD8^+$ lymphoblastic thymic lymphoma without BM invasion (Onoyama et al. 2007), suggesting that the developmental stage at which *Fbxw7* deletion occurs defines T-lineage tumor types; i.e., leukemia versus lymphoma.

To determine whether p53 inactivation promotes leukemogenesis in *Fbxw7*-deficient mice, we generated *p53*$^{-/-}$;*Mx-1-Cre(+);Fbxw7*$^{fl/-}$ mice ($p53^{-/-}$;*Fbxw7*-deficient mice). These mice developed milder anemia and thrombocytopenia than did *Fbxw7*-deficient mice and exhibited considerably greater numbers of peripheral leukocytes after pIpC treatment (Supplemental Fig. S9), indicating that p53-dependent apoptosis contributes to the reduction of *Fbxw7*-deficient BM. All *p53*$^{-/-}$;*Fbxw7*-deficient mice developed T-cell malignancies with a much shorter latency and died within 12 wk, suggesting that a p53-dependent checkpoint suppresses leukemogenesis in *Fbxw7*-deficient mice (Fig. 4F). During our observation of 25 wk, two of 13 *p53*$^{-/-}$ mice died of T-cell thymic lymphoma, but none of them developed T-ALL (data not shown). These findings suggest that deletion of *Fbxw7* provides strong selection of hematopoietic cells that harbor suppressed p53 function. Several studies demonstrate that p53 expression or function is suppressed during tumorigenesis by oncogenes including *Notch* and *c-Myc* (Eischen et al. 1999; Beverly et al. 2005). Eischen et al. (1999) have reported that c-Myc activates the $p19^{Arf}$–Mdm2–p53 tumor suppressor pathway, enhancing p53-dependent apoptosis, and strongly selects for subsequently spontaneous p53 inactivation, resulting in canceling its protective checkpoint function and the occurrence of tumorigenesis, such as lymphoma. These findings support the idea that p53 inactivation is

an essential event in leukemogenesis in *Fbxw7*-deficient hematopoietic cells. Although $p19^{Arf}$, an upstream p53 regulator, was significantly elevated and Mdm2 was reduced, p53 was significantly inactivated in *Fbxw7*-deficient leukemic cells (Supplemental Fig. S10). p53 exerts negative feedback control on $p19^{Arf}$ through its interactor, CARF (Kamrul et al. 2007). Thus, elevated $p19^{Arf}$ protein levels seen in T-ALL cells further support the fact that p53 function is strongly inhibited during leukemogenesis. Although the precise mechanism underlying reduced p53 protein levels remains elusive, p53 degradation via a proteasome-dependent pathway is likely compromised in the absence of Fbxw7. Loss of Fbxw7 also induces genomic instability and genomic alterations (Rajagopalan et al. 2004), which may also initiate leukemogenesis in *Fbxw7*-deficient mice.

These mouse phenotypes led us to analyze *FBXW7* mutations in human T-ALL patients. Mutation of *FBXW7* in the WD40 domain, a crucial site for protein targeting, was observed in eight of 44 cases, and most mutations (seven of eight; 88%) were heterozygous (Supplemental Table S1), suggesting that FBXW7 loss of function is tightly associated with T-ALL development in humans and that *FBXW7* acts in a haplo-insufficient manner as a tumor suppressor gene in humans as in mice. On the other hand, gain-of-function mutations in *NOTCH1* (N-terminal [HD-N] and C-terminal [HD-C] heterodimerization domains and PEST domains) (Weng et al. 2004; Grabher et al. 2006) were observed in 19 of 44 cases. Interestingly, most T-ALL cases with the *FBXW7* mutation (six of eight; 75%) harbored the *NOTCH1* mutations as well, but which mutation is more primary in these T-ALL cases could not be determined sufficiently in the current study. *c-Myc* is a direct Notch1 target in Notch-dependent T-ALL (Weng et al. 2006). Since NOTCH and c-MYC are FBXW7 targets, NOTCH1-independent c-MYC up-regulation could further contribute to leukemogenesis in T-ALL with both *NOTCH1* and *FBXW7* mutations. Moreover, given the two samples with *FBXW7* mutations had wild-type *NOTCH1* (two of eight; 25%), *FBXW7* mutations do not necessarily require the *NOTCH1* mutations as we presented in a mouse model in this study.

This is the first report of *FBXW7* mutations in Japanese T-ALL patients, representing a quite even population compared with the other races that were reported previously. It has been well established that Notch1 gain-of-function mutation is considered as a primary cause to develop T-ALL, because somatic activating mutations of Notch1 have been identified in >50% of all T-ALL cases and are found in all previously defined T-ALL subtypes (Grabher et al. 2006). On the other hand, our analysis in this study revealed that *FBXW7* single mutation was seen in 4.5% (two of 44) of Japanese T-ALL patients. This frequency is slightly lower than that of T-ALL patients in North America: 6.5% (six of 92) (Thompson et al. 2007) and 6.3% (two of 32) (Maser et al. 2007). These findings indicate that there is a genomic type of *FBXW7* single mutation in T-ALL patients infrequently but universally, suggesting the existence of T-ALL that does not bear a *NOTCH1* mutation. We believe that it is noteworthy that we clearly demonstrated, through our analysis of a murine T-ALL model, the mechanism in which *FBXW7* loss of function could be a primary cause for developing T-ALL similar to a *NOTCH1* gain-of-function mutation.

Recently, an array-based comparative genome hybridization (array-CGH) study indicated that *FBXW7* and *PTEN* are commonly mutated in human T-ALL (Maser et al. 2007). It was reported previously that *Pten* deletion induces abnormal active cell cycling of HSCs, leading to their premature loss. *Pten* deletion also results in generation of leukemia-initiating cells. Inhibition of mTOR by rapamycin not only depletes leukemia-initiating cells but also restores normal HSC function (Yilmaz et al. 2006). Similar to *Pten*, *Fbxw7* has distinct effects on normal stem cells and cancer stem cells within the same tissue (Supplemental Fig. S1). Loss-of-function mutations in these genes in normal HSCs are likely prerequisites for generation of cancer stem cells.

Materials and methods

Mx-1-Cre(+);Fbxw7$^{+/-}$ mice were obtained by mating *Fbxw7*$^{+/-}$ mice (Tsunematsu et al. 2004) with interferon-inducible *Mx-1-Cre* transgenic mice. To generate *Mx-1-Cre(+);Fbxw7*$^{fl/-}$ (Fbxw7-deficient) and *Mx-1-Cre(−);Fbxw7*$^{+/fl}$ (control) mice, *Mx-1-Cre(+);Fbxw7*$^{+/-}$ mice were crossed with *Fbxw7*$^{fl/fl}$ mice (Onoyama et al. 2007). To induce *Cre*, mice received 500 μg of pIpC intraperitoneally on three alternate days. C57BL/6-Ly5.1 congenic mice were purchased from Sankyo-Lab Service and C57BL/6-Ly5.1/Ly5.2 F_1 mice were used for competitive reconstitution assays. Animal care was in accordance with the guidance of Keio University for animal and recombinant DNA experiments. See the Supplemental Material for additional procedures.

Acknowledgments

We are grateful to Dr. Klaus Rajewsky (Harvard Medical School) for kindly providing us with *Mx-1-Cre* transgenic mice, and to Dr. Stephen J. Elledge (Harvard Medical School) for helpful advice. We thank Drs. Kristen E. Hurov and Shuhei Matsuoka for critical assistance in manuscript preparation, and A. Ono, K. Fukushima, T. Okawa, and S. Suzuki for technical assistance with the experiments. This work was supported by grants-in-aid for Specially Promoted Research and Scientific Research (C) from the Ministry of Education, Culture, Sports, Science and Technology of Japan.

References

Arai, F., Hirao, A., Ohmura, M., Sato, H., Matsuoka, S., Takubo, K., Ito, K., Koh, G.Y., and Suda, T. 2004. Tie2/angiopoietin-1 signaling regulates hematopoietic stem cell quiescence in the bone marrow niche. *Cell* **118:** 149–161.

Beverly, L.J., Felsher, D.W., and Capobianco, A.J. 2005. Suppression of p53 by Notch in lymphomagenesis: Implications for initiation and regression. *Cancer Res.* **65:** 7159–7168.

Calvi, L.M., Adams, G.B., Weibrecht, K.W., Weber, J.M., Olson, D.P., Knight, M.C., Martin, R.P., Schipani, E., Divieti, P., Bringhurst, F.R., et al. 2003. Osteoblastic cells regulate the haematopoietic stem cell niche. *Nature* **425:** 841–846.

Cheng, T., Rodrigues, N., Shen, H., Yang, Y., Dombkowski, D., Sykes, M., and Scadden, D.T. 2000. Hematopoietic stem cell quiescence maintained by p21cip1/waf1. *Science* **287:** 1804–1808.

Collado, M., Gil, J., Efeyan, A., Guerra, C., Schuhmacher, A.J., Barradas, M., Benguria, A., Zaballos, A., Flores, J.M., Barbacid, M., et al. 2005. Tumour biology: Senescence in premalignant tumours. *Nature* **436:** 642.

Eischen, C.M., Weber, J.D., Roussel, M.F., Sherr, C.J., and Cleveland, J.L. 1999. Disruption of the ARF–Mdm2–p53 tumor suppressor pathway in Myc-induced lymphomagenesis. *Genes & Dev.* **13:** 2658–2669.

Ekholm-Reed, S., Spruck, C.H., Sangfelt, O., van Drogen, F., Mueller-Holzner, E., Widschwendter, M., Zetterberg, A., and Reed, S.I. 2004. Mutation of hCDC4 leads to cell cycle deregulation of cyclin E in cancer. *Cancer Res.* **64:** 795–800.

Fuchs, S.Y. 2005. Tumor suppressor activities of the Fbw7 E3 ubiquitin ligase receptor. *Cancer Biol. Ther.* **4:** 506–508.

Grabher, C., von Boehmer, H., and Look, A.T. 2006. Notch 1 activation in the molecular pathogenesis of T-cell acute lymphoblastic leukaemia. *Nat. Rev. Cancer* **6:** 347–359.

Hock, H., Hamblen, M.J., Rooke, H.M., Schindler, J.W., Saleque, S., Fujiwara, Y., and Orkin, S.H. 2004. Gfi-1 restricts proliferation and preserves functional integrity of haematopoietic stem cells. *Nature* **431:** 1002–1007.

Ito, K., Hirao, A., Arai, F., Matsuoka, S., Takubo, K., Hamaguchi, I., Nomiyama, K., Hosokawa, K., Sakurada, K., Nakagata, N., et al. 2004. Regulation of oxidative stress by ATM is required for self-renewal of haematopoietic stem cells. *Nature* **431:** 997–1002.

Kamrul, H.M., Wadhwa, R., and Kaul, S.C. 2007. CARF binds to three members (ARF, p53, and HDM2) of the p53 tumor-suppressor pathway. *Ann. N. Y. Acad. Sci.* **1100:** 312–315.

Look, A.T. 2004. Molecular pathways in T-cell acute lympho-blastic leukemia: Ramifications for therapy. *Clin. Adv. Hematol. Oncol.* **2:** 779–780.

Mao, J.H., Perez-Losada, J., Wu, D., Delrosario, R., Tsunematsu, R., Nakayama, K.I., Brown, K., Bryson, S., and Balmain, A. 2004. Fbxw7/Cdc4 is a p53-dependent, haploinsufficient tumour suppressor gene. *Nature* **432:** 775–779.

Maser, R.S., Choudhury, B., Campbell, P.J., Feng, B., Wong, K.K., Protopopov, A., O'Neil, J., Gutierrez, A., Ivanova, E., Perna, I., et al. 2007. Chromosomally unstable mouse tumours have genomic alterations similar to diverse human cancers. *Nature* **447:** 966–971.

Minella, A.C. and Clurman, B.E. 2005. Mechanisms of tumor suppression by the SCF(Fbw7). *Cell Cycle* **4:** 1356–1359.

Nakayama, K.I. and Nakayama, K. 2006. Ubiquitin ligases: Cell-cycle control and cancer. *Nat. Rev. Cancer* **6:** 369–381.

Onoyama, I., Tsunematsu, R., Matsumoto, A., Kimura, T., de Alboran, I.M., Nakayama, K., and Nakayama, K.I. 2007. Conditional inactivation of Fbxw7 impairs cell-cycle exit during T cell differentiation and results in lymphomatogenesis. *J. Exp. Med.* **204:** 2875–2888.

Pui, J.C., Allman, D., Xu, L., DeRocco, S., Karnell, F.G., Bakkour, S., Lee, J.Y., Kadesch, T., Hardy, R.R., Aster, J.C., et al. 1999. Notch1 expression in early lymphopoiesis influences B versus T lineage determination. *Immunity* **11:** 299–308.

Rajagopalan, H., Jallepalli, P.V., Rago, C., Velculescu, V.E., Kinzler, K.W., Vogelstein, B., and Lengauer, C. 2004. Inactivation of hCDC4 can cause chromosomal instability. *Nature* **428:** 77–81.

Spruck, C.H., Strohmaier, H., Sangfelt, O., Muller, H.M., Hubalek, M., Muller-Holzner, E., Marth, C., Widschwendter, M., and Reed, S.I. 2002. hCDC4 gene mutations in endometrial cancer. *Cancer Res.* **62:** 4535–4539.

Tetzlaff, M.T., Yu, W., Li, M., Zhang, P., Finegold, M., Mahon, K., Harper, J.W., Schwartz, R.J., and Elledge, S.J. 2004. Defective cardiovascular development and elevated cyclin E and Notch proteins in mice lacking the Fbw7 F-box protein. *Proc. Natl. Acad. Sci.* **101:** 3338–3345.

Thompson, B.J., Buonamici, S., Sulis, M.L., Palomero, T., Vilimas, T., Basso, G., Ferrando, A., and Aifantis, I. 2007. The SCFFBW7 ubiquitin ligase complex as a tumor suppressor in T cell leukemia. *J. Exp. Med.* **204:** 1825–1835.

Tothova, Z., Kollipara, R., Huntly, B.J., Lee, B.H., Castrillon, D.H., Cullen, D.E., McDowell, E.P., Lazo-Kallanian, S., Williams, I.R., Sears, C., et al. 2007. FoxOs are critical mediators of hematopoietic stem cell resistance to physiologic oxidative stress. *Cell* **128:** 325–339.

Tsunematsu, R., Nakayama, K., Oike, Y., Nishiyama, M., Ishida, N., Hatakeyama, S., Bessho, Y., Kageyama, R., Suda, T., and Nakayama, K.I. 2004. Mouse Fbw7/Sel-10/Cdc4 is required for notch degradation during vascular development. *J. Biol. Chem.* **279:** 9417–9423.

Welchman, R.L., Gordon, C., and Mayer, R.J. 2005. Ubiquitin and ubiquitin-like proteins as multifunctional signals. *Nat. Rev. Mol. Cell Biol.* **6:** 599–609.

Weng, A.P., Ferrando, A.A., Lee, W., Morris, J.P.t., Silverman, L.B., Sanchez-Irizarry, C., Blacklow, S.C., Look, A.T., and Aster, J.C. 2004. Activating mutations of NOTCH1 in human T cell acute lymphoblastic leukemia. *Science* **306:** 269–271.

Weng, A.P., Millholland, J.M., Yashiro-Ohtani, Y., Arcangeli, M.L., Lau, A., Wai, C., Del Bianco, C., Rodriguez, C.G., Sai, H., Tobias, J., et al. 2006. c-Myc is an important direct target of Notch1 in T-cell acute lymphoblastic leukemia/lymphoma. *Genes & Dev.* **20:** 2096–2109.

Wilson, A., Murphy, M.J., Oskarsson, T., Kaloulis, K., Bettess, M.D., Oser, G.M., Pasche, A.C., Knabenhans, C., Macdonald, H.R., and Trumpp, A. 2004. c-Myc controls the balance between hematopoietic stem cell self-renewal and differentiation. *Genes & Dev.* **18:** 2747–2763.

Yilmaz, O.H., Valdez, R., Theisen, B.K., Guo, W., Ferguson, D.O., Wu, H., and Morrison, S.J. 2006. Pten dependence distinguishes haematopoietic stem cells from leukaemia-initiating cells. *Nature* **441:** 475–482.

Zhang, J., Niu, C., Ye, L., Huang, H., He, X., Tong, W.G., Ross, J., Haug, J., Johnson, T., Feng, J.Q., et al. 2003. Identification of the haematopoietic stem cell niche and control of the niche size. *Nature* **425:** 836–841.

Zhang, J., Grindley, J.C., Yin, T., Jayasinghe, S., He, X.C., Ross, J.T., Haug, J.S., Rupp, D., Porter-Westpfahl, K.S., Wiedemann, L.M., et al. 2006. PTEN maintains haematopoietic stem cells and acts in lineage choice and leukaemia prevention. *Nature* **441:** 518–522.

Zindy, F., Eischen, C.M., Randle, D.H., Kamijo, T., Cleveland, J.L., Sherr, C.J., and Roussel, M.F. 1998. Myc signaling via the ARF tumor suppressor regulates p53-dependent apoptosis and immortalization. *Genes & Dev.* **12:** 2424–2433.

ELSEVIER

Cancer Genetics and Cytogenetics 186 (2008) 115–119

CANCER GENETICS AND CYTOGENETICS

Short communication

MNX1–ETV6 fusion gene in an acute megakaryoblastic leukemia and expression of the *MNX1* gene in leukemia and normal B cell lines

Takeshi Taketani[a,b], Tomohiko Taki[c], Masahiro Sako[d], Takefumi Ishii[d], Seiji Yamaguchi[a], Yasuhide Hayashi[e,*]

[a]*Department of Pediatrics, Shimane University Faculty of Medicine, Izumo, Shimane, Japan*
[b]*Division of Blood Transfusion, Shimane University Hospital, Matsue, Shimane, Japan*
[c]*Department of Molecular Laboratory Medicine, Kyoto Prefectural University of Medicine Graduate School of Medical Science, Kyoto, Japan*
[d]*Department of Pediatric Hematology/Oncology, Osaka City General Hospital, Osaka, Japan*
[e]*Department of Hematology/Oncology, Gunma Children's Medical Center, 779 Shimohakoda, Hokkitsu, Shibukawa, Gunma 377-8577, Japan*

Received 5 March 2008; received in revised form 11 June 2008; accepted 27 June 2008

Abstract Patients with infant acute myeloid leukemia (AML) who carry a t(7;12)(q36;p13) translocation have been reported to have a poor clinical outcome. *MNX1–ETV6* fusion transcripts (previously *HLXB9–ETV6*) were rarely detected in AML patients having t(7;12)(q36;p13). A 23-month-old girl with acute megakaryoblastic leukemia (AMKL) exhibited chromosome abnormalities, including add(7)(q22), and del(12)(p12p13). Southern blot analysis of bone marrow cells showed an *ETV6* gene rearrangement. Reverse transcriptase-polymerase chain reaction (RT-PCR) followed by sequence analysis revealed the presence of an *MNX1–ETV6* fusion gene. The patient responded well to chemotherapy, achieved complete remission, and at writing had been in complete remission for 60 months. The *MNX1* expression by RT-PCR was significantly more frequent in Epstein–Barr virus–transformed B-cell lines derived from normal adult lymphocytes than in leukemic cell lines. This represents a novel case of an AMKL patient with *MNX1–ETV6* fusion transcripts who had a good prognosis.

1. Introduction

Many recurrent chromosomal translocations are involved in acute myeloid leukemia (AML) [1]. AML with 12p13 translocations have been reported to involve the ETS variant gene 6 (*TEL* oncogene) (*ETV6*) [2]. In cases of AML carrying 12p13 abnormalities, a recurrent translocation t(7;12)(q36;p13) is found in 20%–30% of infant cases [3–5]. Fluorescence in situ hybridization assay is needed to evaluate this translocation, because it is difficult to detect by conventional karyotyping [3–5]. AML patients with this translocation are characterized by age under 20 months at diagnosis, thrombocytosis, high percentage of CD34-positive cells, presence of additional chromosomal abnormalities, including trisomy 19 or trisomy 8 (or both), and a poor prognosis [3–5]. An *MNX1–ETV6* fusion gene (previously *HLXB9–ETV6*) was identified in two pediatric AML patients having t(7;12)(q36;p13) [6]; however, heterogeneity of the 7q36 and 12p13 translocations was reported [5,7,8]. Thus, *MNX1–ETV6* fusion gene in AML patients having t(7;12) is infrequently reported [7,8].

We describe the case of a 23-month-old AML patient with add(7)(q22), del(12)(p12p13), and *MNX1–ETV6* fusion transcript; the child has remained alive for 5 years. We also report the expression of the *MNX1* gene in several leukemic and normal Epstein–Barr virus-transformed cell lines.

2. Case report

A 23-month-old girl was admitted to Osaka City General Hospital because of appetite loss and pallor. Blood examination showed a white blood cell count of 10,520/μL with 55.5% blasts, a hemoglobin level of 7.0 g/dL, and a platelet count of 164,000/μL. She had a mediastinal mass, but no hepatosplenomegaly. Bone marrow examination revealed a nuclear cell count of 30,000/μL with 71.2% blasts. The

* Corresponding author. Tel.: +81-279-52-3551, ext. 2200; fax: +81-279-52-2045.
E-mail address: hayashiy-tky@umin.ac.jp (Y. Hayashi).

0165-4608/08/$ – see front matter
doi:10.1016/j.cancergencyto.2008.06.009

blasts were negative for myeloperoxidase staining and platelet peroxidase staining electron-microscopically. Flow cytometric analysis showed that the blasts expressed CD41, CD36, CD13, CD33, CD15, and CD7 antigens, suggesting megakaryoblastic origin. Conventional G-banding chromosomal analysis revealed a karyotype of 46,XX,add (7)(q22),del(12)(p12p13) in all 20 bone marrow cells examined (Fig. 1).

The patient was diagnosed as having AMKL (M7 subtype, based on the French–American–British classification), and was treated on the Japanese Childhood AML Cooperative Study Group Protocol, AML99 [9]. She obtained complete remission with induction chemotherapy (cytarabine, etoposide, and mitoxantrone). Thereafter, she was treated with five additional courses of intensive chemotherapy (high-dose cytarabine, etoposide, idarubicin, and mitoxantrone). As of writing, she had been in complete remission for 60 months after diagnosis.

3. Materials and methods

3.1. Southern blot analysis

High molecular weight DNA was extracted from bone marrow cells of the patient by proteinase K digestion and phenol–chloroform extraction [10]. Ten micrograms of DNA was digested with *Eco*RI, subjected to electrophoresis on 0.7% agarose gels, and transferred to nylon membrane, and hybridized to cDNA probes ^{32}P-labeled by the random hexamer method [10]. The probes used were a 516-bp *MNX1* cDNA fragment (nucleotide nt598 to nt1114; GenBank accession no. NM_005515; previously *HLXB9*).

3.2. Expression of WT1 mRNA and mutation of FLT3

WT1 mRNA was examined for detection of minimal residual disease as previously reported [11]. Internal tandem duplication and mutation of *FLT3* were examined as previously reported [10].

3.3. Reverse transcriptase–polymerase chain reaction and nucleotide sequencing

MNX1–ETV6 chimeric mRNA was detected by reverse transcriptase–polymerase chain reaction (RT-PCR) as described previously [12]. Total RNA was extracted from the leukemic cells of the patient using the acid guanidine thiocyanate–phenol chloroform method [12]. Total RNA (4 μg) was reverse-transcribed to cDNA, using a cDNA synthesis kit (GE Healthcare Bio-Science, Piscataway, NJ) [12]. PCR was performed with AmpliTaq Gold DNA polymerase (Applied Biosystems, Foster City, CA; Tokyo, Japan), using the reagents recommended by the manufacturer. The primers used and PCR conditions were as described previously [6]. The PCR products were subcloned into pCR2.1 vector (Invitrogen, Carlsbad, CA) and sequenced by the fluorometric method using the BigDye Terminator cycle sequencing kit (Applied Biosystems).

3.4. Expression of the MNX1 gene by RT-PCR in leukemic cell lines

To analyze the expression pattern of the *MNX1* gene in leukemic cell lines, RT-PCR was performed. Fifty-nine cell lines were examined, as follows [12]; 10 B-precursor ALL cell lines (LC4-1, NALM-6, NALM-24, NALM-26, UTP-2, RS4;11, SCMC-L10, KOCL-33, KOCL-45, KOCL-69), 9

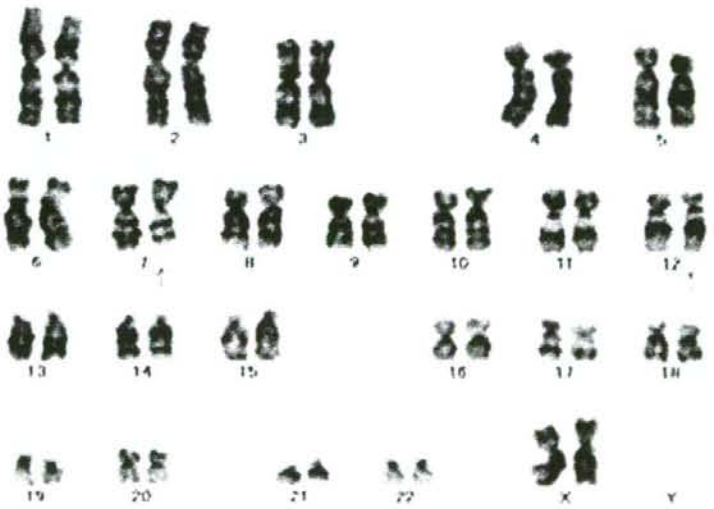

Fig. 1. G-banding karyotype of the leukemic cells in a pediatric patient with acute megakaryoblastic leukemia: 46,XX,add(7)(q22),del(12)(p12p13).

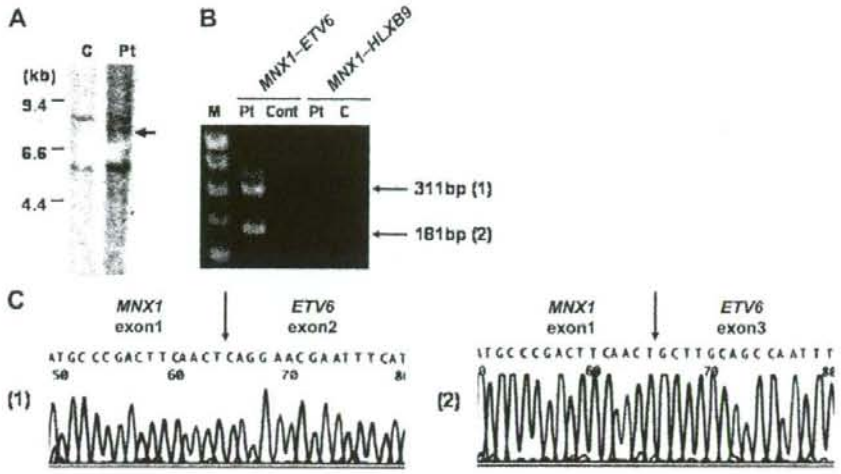

Fig. 2. Detection of the *MNX1–ETV6* fusion gene (previously *HLXB9–ETV6*). (A) Rearrangement of the *MNX1* gene by Southern blotting with *Eco*RI digestion. The arrow indicates a rearranged band of the *MNX1* gene; C, control; Pt, patient. (B) The *MNX1–ETV6* fusion transcript identified by reverse transcriptase–polymerase chain reaction (RT-PCR). Lanes 2 and 3, *MNX1–ETV6* fusion transcript; lanes 4 and 5, *ETV6–MNX1* fusion transcript. C, control; M, size marker; Pt, patient; (C) Nucleotide and amino acid sequencing of two *MNX1–ETV6* fusion transcripts.

B-ALL cell lines (BALM-1, BALM-13, BALM-14, BJAB, DAUDI, RAJI, RAMOS, BAL-KH, NAMALLA), 9 T-ALL cell lines (RPMI-8402, MOLT-14, THP-6, PEER, H-SB2, HPB-ALL, L-SAK, L-SMY, KCMC-T), 8 AML cell lines (YNH-1, ML-1, KASUMI-3, KG-1, inv-3, SN-1, NB4, HEL), 6 acute monocytic leukemia cell lines (THP-1, IMS/M1, CTS, P31/FUJ, MOLM-13, KOCL-48), 5 chronic myelogenous leukemia cell lines (MOLM-1, MOLM-7, TS9;22, SS9;22, K-562), 2 acute megakaryoblastic leukemia cell lines (CMS, CMY), and 10 Epstein-Barr virus transformed B lymphocyte (EBV-B) cell lines derived from normal adult peripheral lymphocytes. Five normal BM samples were also examined. RT-PCR mixtures and conditions were the same as described [10]. The primers used for RT-PCR were HLXB9-658F (5′-GGCATGATCCTGCC-TAAGAT-3′) (sense primer) and HLXB9-1092R (TGCT GTAGGGGAAATGGTCGTCG) (antisense primer) [6].

4. Results and discussion

The karyotype of the patient's leukemic cells was 46,XX,add(7)(q22),del(12)(p12p13), suggesting that both *ETV6* and *MNX1* were involved in this chromosomal abnormality. With informed consent from the patient's parents, DNA and total RNA were extracted from bone marrow cells of the patient. Southern blot analysis of DNA from leukemic cells of the patient using the *MNX1* probe showed a rearranged band (Fig. 2A). We performed RT-PCR for *MNX1–ETV6* chimeric mRNA and obtained two RT-PCR products, of 311 bp and 181 bp (Fig. 2B). Sequence analysis of these PCR products showed that one product was an in-frame fusion transcript of exon 1 of *MNX1* to exon 3 of *ETV6*, and the other was an out-of-frame fusion transcript of exon 1 of *MNX1* to exon 2 of *ETV6* (Fig. 2C). These transcripts were the same as previously reported [6]. The reciprocal *ETV6–MNX1* transcript was not detected (Fig. 2B).

The *WT1* mRNA level was 3,400 copies/μg RNA at diagnosis, but decreased to <50 copies/μg RNA after remission. Neither internal tandem duplication nor mutation of *FLT3* were found in this patient, suggesting that the prognosis is not poor [1].

Table 1
Expression of the *MNX1* gene in leukemia and EBV-B cell lines by reverse transcriptase–polymerase chain reaction

Cell line	Cells examined, no.	Cells expressing *MNX1*, no. (%)
ALL	28	5 (17.9)
B precursor	10	0 (0)
B	9	2 (22.2)
T	9	3 (33.3)
AML	16	3 (18.8)
AML	8	1 (12.5)
AMoL	6	2 (33.3)
AMKL	2	0 (0)
CML	5	1 (20)
EBV-B	10	7 (70)
normal BM	5	0 (0)

Abbreviations: ALL, acute lymphoblastic leukemia; AMKL, acute megakaryoblastic leukemia; AML, acute myeloid leukemia; AMoL, acute monocytic leukemia; B, B-cell; BM, bone marrow; CML, chronic myelogenous leukemia; EBV-B, Epstein–Barr virus-transformed human B lymphocytes; T, T-cell.

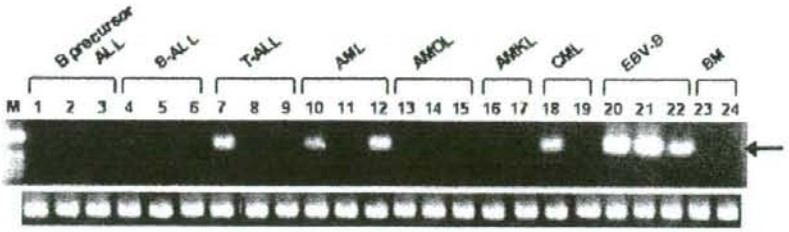

Fig. 3. Expression of the *MNX1* gene in leukemia and EBV-B cell lines by RT-PCR. ALL, acute lymphoblastic leukemia; AMKL, acute megakaryoblastic leukemia; AML, acute myeloid leukemia; AMOL, acute monocytic leukemia; B, B-cell; BM, bone marrow; CML, chronic myelogenous leukemia; EBV-B, Epstein–Barr virus-transformed human B lymphocytes; T, T-cell.

We next examined the *MNX1* expression by RT-PCR analysis in 49 leukemic cell lines, and 10 EBV-B cell lines. *MNX1* was not frequently expressed in lymphoid or myeloid leukemic cell lines (Table 1; Fig. 3). *MNX1* was expressed in 7 of 10 EBV-B cell lines, but not in 5 normal BM cells. The *MNX1* expression was significantly more frequent in EBV-B cell lines than in leukemic cell lines ($P = 0.0015$) or in normal BM cells ($P = 0.0256$). The *MNX1* was frequently expressed in CD34-positive cells purified from normal BM cells, acute leukemia cells, and AML cells having t(7;12)(q36;p13) [5,13,14]. It is unknown whether the incidence of *MNX1* expression differs among leukemia cell lines. Mature B-lineage cells are likely to frequently express *MNX1* transcripts, and the transcripts were more prevalent in several human B lineage cell line and tonsil B cells [15]. The present findings are compatible with previous reports. *MNX1* may be associated with differentiation of B cells.

MNX1–ETV6 fusion transcript has so far been detected in only four out of the many AML patients who carry the t(7;12) anomaly [5,6]. Difficulty of detection of this fusion transcript is due to breakpoint heterogeneity of the 7q36 and 12p13 in this translocation [7,8]. Clinical features of AML patients having t(7;12) did not differ between the presence and absence of *MNX1–ETV6* fusion transcripts [5]. Notably, clinical characteristics of the present patient were different from those of AML patients having t(7;12) previously reported. Our patient was diagnosed as having AMKL, although most AML patients having t(7;12) were identified as poorly differentiated FAB subtypes [5]. Only one patient was reported to be diagnosed with AMKL; however, *MNX1–ETV6* fusion transcript was not examined in that case [4]. An additional cytogenetic abnormality is trisomy 19 [3–5]. Chromosomal analysis of the present patient showed absence of additional chromosomal abnormalities, suggesting long-term disease-free survival with chemotherapy alone. All AML patients, except one who had both t(7;12) and trisomy 19, died [3–6]. These findings suggest that t(7;12) is associated only with leukemogenesis, and that other factors including trisomy 19 and *FLT3* mutations, may affect the prognosis of AML patients having t(7;12).

In conclusion, an AMKL patient with *MNX1–ETV6* fusion transcripts had a good prognosis. Further accumulation of clinical and molecular data of AML patients having t(7;12) is needed to clarify this result.

Acknowledgments

We express our appreciation to Mrs. Shoko Sohma and Hisae Soga for their excellent technical assistance. We thank Dr. Takeyuki Sato, Department of Pediatrics, Chiba University School of Medicine, Japan, for providing AMKL (CMS, CMY) cell lines; Dr. Kanji Sugita, Department of Pediatrics, Yamanashi University School of Medicine, Japan, for providing ALL (KOCL-33, -45, -69) cell lines and AMoL (KOCL-48) cell lines; and Dr. Yoshinobu Matsuo, Hayashibara Biochemical Laboratories, Inc., Fujisaki Cell Center, Japan, for providing varieties of ALL cell lines. This work was supported by a Grant-in-Aid for Cancer Research, Research on Children and Families from the Ministry of Health, Labor, and Welfare of Japan, a Grant-in-Aid for Scientific Research (C), and Exploratory Research from the Ministry of Education, Culture, Sports, Science, and Technology of Japan.

References

[1] Hayashi Y. The molecular genetics of recurring chromosome abnormalities in acute myeloid leukemia. Semin Hematol 2000;37:368–80.

[2] Bohlander SK. *ETV6*: a versatile player in leukemogenesis. Semin Cancer Biol 2005;15:162–74.

[3] Tosi S, Harbott J, Teigler-Schlegel A, Haas OA, Pirc-Danoewinata H, Harrison CJ, Biondi A, Cazzaniga G, Kempski H, Scherer SW, Kearney L. t(7;12)(q36;p13), a new recurrent translocation involving *ETV6* in infant leukemia. Genes Chromosomes Cancer 2000;29:325–32.

[4] Slater RM, von Drunen E, Kroes WG, Weghuis DO, van den Berg E, Smit EM, van der Does-van den Berg A, van Wering E, Hählen K, Carroll AJ, Raimondi SC, Beverloo HB. t(7;12)(q36;p13) and t(7;12)(q32;p13): translocations involving *ETV6* in children 18 months of age or younger with myeloid disorders. Leukemia 2001;15:915–20.

[5] von Bergh AR, van Drunen E, van Wering ER, van Zutven LJ, Hainmann I, Lönnerholm G, Meijerink JP, Pieters R, Beverloo HB.

High incidence of t(7;12)(q36;p13) in infant AML but not in infant ALL with a dismal outcome and ectopic expression of *HLXB9*. Genes Chromosomes Cancer 2006;45:731–9.

[6] Beverloo HB, Panagopoulos I, Isaksson M, van Wering E, van Drunen E, de Klein A, Johansson B, Slater R. Fusion of the homeobox gene *HLXB9* and the *ETV6* gene in infant acute myeloid leukemias with the t(7;12)(q36;p13). Cancer Res 2001;61:5374–7.

[7] Simmons HM, Oseth L, Nguyen P, O'Leary M, Conklin KF, Hirsch B. Cytogenetic and molecular heterogeneity of 7q36/12p13 rearrangements in childhood AML. Leukemia 2002;16:2408–16.

[8] Tosi S, Hughes J, Scherer SW, Nakabayashi K, Harbott J, Haas OA, Cazzaniga G, Biondi A, Kempski H, Kearney L. Heterogeneity of the 7q36 breakpoints in the t(7;12) involving *ETV6* in infant leukemia. Genes Chromosomes Cancer 2003;38:191–200.

[9] Shimada A, Taki T, Tabuchi K, Tawa A, Horibe K, Tsuchida M, Hanada R, Tsukimoto I, Hayashi Y. *KIT* mutations, and not *FLT3* internal tandem duplication, are strongly associated with a poor prognosis in pediatric acute myeloid leukemia with t(8;21): a study of the Japanese Childhood AML Cooperative Study Group. Blood 2006;107:1806–9.

[10] Taketani T, Taki T, Sugita K, Furuichi Y, Ishii E, Hanada R, Tsuchida M, Sugita K, Ida K, Hayashi Y. *FLT3* mutations in the activation loop of tyrosine kinase domain are frequently found in infant ALL with *MLL* rearrangements and pediatric ALL with hyperdiploidy. Blood 2004;103:1085–8.

[11] Inoue K, Ogawa H, Yamagami T, Soma T, Tani Y, Tatekawa T, Oji Y, Tamaki H, Kyo T, Dohy H, Hiraoka A, Masaoka T, Kishimoto T, Sugiyama H. Long-term follow-up of minimal residual disease in leukemia patients by monitoring *WT1* (Wilms tumor gene) expression levels. Blood 1996;88:2267–78.

[12] Taketani T, Taki T, Shibuya N, Kikuchi A, Hanada R, Hayashi Y. Novel *NUP98–HOXC11* fusion gene resulted from a chromosomal break within exon 1 of *HOXC11* in acute myeloid leukemia with t(11;12)(p15;q13). Cancer Res 2002;62:4571–4.

[13] Deguchi Y, Kehrl JH. Selective expression of two homeobox genes in CD34-positive cells from human bone marrow. Blood 1991;78:323–8.

[14] Deguchi Y, Yamanaka Y, Theodossiou C, Najfeld V, Kehrl JH. High expression of two diverged homeobox genes, HB24 and HB9, in acute leukemias: molecular markers of hematopoietic cell immaturity. Leukemia 1993;7:446–51.

[15] Harrison KA, Druey KM, Deguchi Y, Tuscano JM, Kehrl JH. A novel human homeobox gene distantly related to proboscipedia is expressed in lymphoid and pancreatic tissues. J Biol Chem 1994;269:19968–75.

Oncogene (2008) 27, 2249–2256

www.nature.com/onc

ONCOGENOMICS

Identification of the novel *AML1* fusion partner gene, *LAF4*, a fusion partner of *MLL*, in childhood T-cell acute lymphoblastic leukemia with t(2;21)(q11;q22) by bubble PCR method for cDNA

Y Chinen[1,2], T Taki[1], K Nishida[2], D Shimizu[2], T Okuda[2], N Yoshida[2], C Kobayashi[3], K Koike[3], M Tsuchida[3], Y Hayashi[4] and M Taniwaki[1,2]

[1]*Department of Molecular Laboratory Medicine, Kyoto Prefectural University of Medicine Graduate School of Medical Science, Kamigyo-ku, Kyoto, Japan;* [2]*Department of Molecular Hematology and Oncology, Kyoto Prefectural University of Medicine Graduate School of Medical Science, Kamigyo-ku, Kyoto, Japan;* [3]*Department of Pediatrics, Ibaraki Children's Hospital, Futabadai, Mito, Japan and* [4]*Gunma Children's Medical Center, Shimohakoda, Hokkitsu, Shibukawa, Gunma, Japan*

The *AML1* gene is frequently rearranged by chromosomal translocations in acute leukemia. We identified that the *LAF4* gene on 2q11.2–12 was fused to the *AML1* gene on 21q22 in a pediatric patient having T-cell acute lymphoblastic leukemia (T-ALL) with t(2;21)(q11;q22) using the bubble PCR method for cDNA. The genomic break points were within intron 7 of *AML1* and of *LAF4*, resulting in the in-frame fusion of exon 7 of *AML1* and exon 8 of *LAF4*. The *LAF4* gene is a member of the *AF4/FMR2* family and was previously identified as a fusion partner of *MLL* in B-precursor ALL with t(2;11)(q11;q23), although *AML1-LAF4* was in T-ALL. *LAF4* is the first gene fused with both *AML1* and *MLL* in acute leukemia. Almost all *AML1* translocations except for *TEL-AML1* are associated with myeloid leukemia; however, *AML1-LAF4* was associated with T-ALL as well as *AML1-FGA7* in t(4;21)(q28;q22). These findings provide new insight into the common mechanism of *AML1* and *MLL* fusion proteins in the pathogenesis of ALL. Furthermore, we successfully applied bubble PCR to clone the novel *AML1-LAF4* fusion transcript. Bubble PCR is a powerful tool for detecting unknown fusion transcripts as well as genomic fusion points.

Oncogene (2008) **27,** 2249–2256; doi:10.1038/sj.onc.1210857; published online 29 October 2007

Keywords: *AML1/RUNX1*; *LAF4*; T-cell acute lymphoblastic leukemia; *MLL*

Correspondence: Dr T Taki, Department of Molecular Laboratory Medicine, Kyoto Prefectural University of Medicine Graduate School of Medical Science, 465 Kajii-cho Kawaramachi-Hirokoji, Kamigyo-ku, Kyoto 602-8566, Japan.
E-mail: taki-t@umin.net
Received 4 May 2007; revised 13 September 2007; accepted 17 September 2007; published online 29 October 2007

Introduction

A large number of leukemias have been found to be associated with specific chromosomal aberrations. Recent studies have demonstrated that several chromosomal rearrangements and molecular abnormalities are strongly associated with distinct clinical subgroups and can predict clinical features and therapeutic responses (Rowley, 1999; Taki and Taniwaki, 2006). Some genes have been associated with recurrent rearrangements and have many fusion partner genes, such as *MLL* at 11q23, *TEL (ETV6)* at 12p13 and *NUP98* at 11p15; *AML1* (*RUNX1*, *CBFA2*) at 21q22 is one of the most frequent targets of these chromosomal rearrangements in both acute lymphoblastic leukemia (ALL) and acute myeloid leukemia (AML) (Miyoshi *et al.*, 1991; Hayashi, 2000; Kurokawa and Hirai, 2003). To date, a number of in-frame fusion partners of *AML1* have been cloned: *YTHDF2* at 1p35 (Nguyen *et al.*, 2006), *ZNF687* at 1q21.2 (Nguyen *et al.*, 2006), *MDS1/EVI1* at 3q26 (Mitani *et al.*, 1994), *FGA7* at 4q28 (Mikhail *et al.*, 2004), *SH3D19* at 4q31.3 (Nguyen *et al.*, 2006), *USP42* at 7p22 (Paulsson *et al.*, 2006), *MTG8* (*ETO*, *CBFA2T1*) at 8q22 (Erickson *et al.*, 1992; Miyoshi *et al.*, 1993), *FOG2* at 8q23 (Chan *et al.*, 2005), *TRPS1* at 8q24 (Asou *et al.*, 2007), *TEL* (*ETV6*) at 12p13 (Golub *et al.*, 1995), *MTG16* at 16q24 (Gamou *et al.*, 1998) and *PRDX4* at Xp22 (Zhang *et al.*, 2004). Most *AML1* translocations, except for *TEL-AML1*, are associated with AML, involving the N-terminus Runt domain and lacking the C-terminus transactivation domain (Kurokawa and Hirai, 2003). AML1 fusion proteins are associated with leukemogenesis by dominantly interfering with normal *AML1*-mediated transcription and acting as a transcriptional repressor (Okuda *et al.*, 1998; Wang *et al.*, 1998). Clinically, patients with AML harboring t(8;21) in both children and adults show a high rate of complete remission, and its prognosis is considered better than that of patients with a normal karyotype or other chromosomal aberrations (Grimwade *et al.*, 1998).

In the present study, we analysed pediatric T-ALL with t(2;21)(q11;q22) and identified the *LAF4* gene,

which is one of the fusion partners of *MLL*, as a novel fusion partner of the *AML1* gene.

Results

Case report

A 6-year-old boy with a high leukocyte count (64 700 μl^{-1}), containing 84% blasts in peripheral blood and with a mediastinal mass, was diagnosed as having T-ALL. A bone marrow smear was hypercellular with 69% blasts and negative for myeloperoxidase. The leukemic cells, after gating of CD45-positive cells, were positive for CD5 (90.7%), CD7 (90.7%), CD58 (69.9%) and cytoplasmic CD3 (92.8%), and negative for HLA-DR, IgG, IgM, Igκ, Igλ, CD8, CD13, CD14, CD19, CD20 and CD33. He was treated on the Tokyo Children's Cancer Study Group (TCCSG) L04-16 extremely high-risk (HEX) protocol, including stem cell transplantation, because the response to initial 7-day prednisolone (60 mg m^{-2}) monotherapy was poor. He achieved complete remission after the induction phase. After the early consolidation phase and two courses of the consolidation phase, he received allogeneic bone marrow transplantation from an unrelated HLA-matched donor 4 months after diagnosis. He has been in complete remission for 17 months.

The patient's leukemic cells at diagnosis were analysed after written informed consent was obtained from his parents, and the ethics committee of Kyoto Prefectural University of Medicine approved this study.

Identification of the AML1-LAF4 *fusion transcript*

Cytogenetic analysis of the leukemic cells of the patient using routine G-banding revealed 47, XY, add(1)(p36), + der(2)t(2;21)(q13;q22), t(2;21)(q13;q22), −9, −9, + mar1, + mar2, and spectral karyotyping (SKY) analysis revealed 47, XY, der(1)t(1;17)(p36.1;q23), der(2)t(2;21)(q11.2;q22), + der(2)t(2;21)(q11.2;q22), del(5)(p15.1), del(9)(q22), del(9)(p13), der(21)t(2;21)(q11.2;q22) (Supplementary Figure S1). Since *AML1* is located at 21q22, we inferred that *AML1* was rearranged in this case. Fluorescence *in situ* hybridization analysis using *AML1*-specific BAC (bacterial artificial chromosome) clones showed split signals of *AML1* on two der(2)t(2;21)(q11.2;q22) and der(21)t(2;21)(q11.2;q22) chromosomes (Figure 1a).

To isolate fusion transcripts of *AML1*, we performed the bubble PCR method for cDNA (Figure 2) and obtained various-sized products (Figure 3a). Four different-sized products were sequenced and two products contained *AML1* sequences fused to unknown sequences. Basic local alignment search tool (BLAST) search revealed that the unknown sequences were part of the *LAF4* gene and both products had the same in-frame junctions (Figure 3b). *LAF4* was located on chromosome 2q11.2–12, which was compatible with the result of spectral karyotyping analysis. We next performed reverse transcription-PCR to confirm *AML1-LAF4* fusion transcripts, and obtained three different-sized *AML1-LAF4* fusion products, including only one in-frame product (Figures 3c and d); however, reciprocal *LAF4-AML1* fusion transcripts were not generated (Figure 3c). Type 2 transcript is an out-of-frame fusion and generated premature termination in exon 9 of *LAF4* (Figure 3d). On the other hand, type 3 transcript is an in-frame fusion of exon 7 of *AML1* and exon 8 of *LAF4*, the same as the type 1 transcript; however, the type 3 transcript contained an 85-bp intronic sequence between exons 9 and 10 of *LAF4*, which might be due to splicing error, and appeared as a premature termination codon within the intronic sequences (Figure 3d). *AML1-LAF4* fusions were also confirmed by fluorescence *in situ* hybridization analysis (Figure 1b).

Detection of AML1-LAF4 *genomic junctions*

Southern blot analysis using a cDNA probe within exon 7 of *AML1* detected a rearranged band derived from an

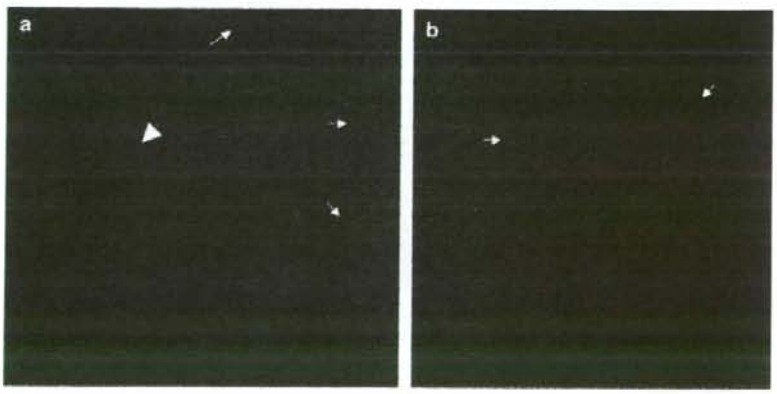

Figure 1 Fluorescence *in situ* hybridization analysis of the leukemic metaphase. **(a)** Both RP11-272A3 (green, 3′ side of *AML1*) and RP11-994N6 (red, 5′ side of *AML1*) were hybridized to normal chromosome 21 (arrowhead), RP11-272A3 to der(21)t(2;21)(q11.2;q22) (arrow, green signal) and RP11-994N6 to two der(2)t(2;21)(q11.2;q22) chromosomes (arrows, red signal). **(b)** Two fusion signals of RP11-994N6 (5′ of *AML1*, red signals) and RP11-527J8 (3′ of *LAF4*, green signals) were detected on two der(2)t(2;21)(q11.2;q22) chromosomes (arrows).

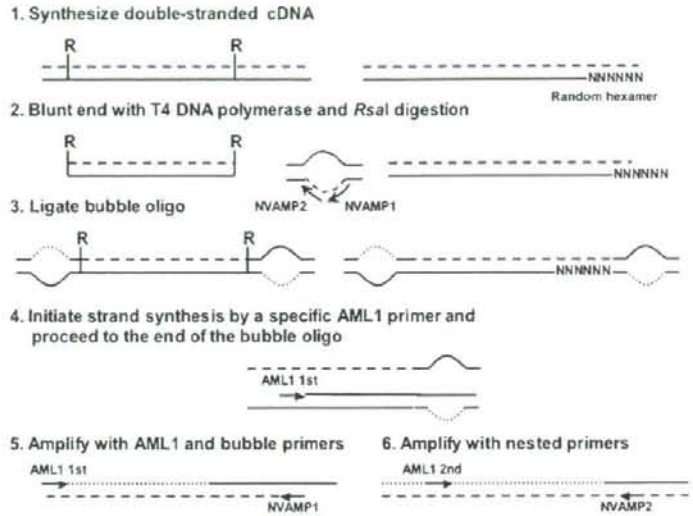

Figure 2 Outline of bubble PCR for cDNA. Bubble PCR primers (NVAMP-1 and NVAMP-2) can only anneal with one complementary sequence for bubble oligo synthesized with *AML1* primer, but not bubble oligo itself; therefore, this single-stranded bubble provides the specificity of the reaction.

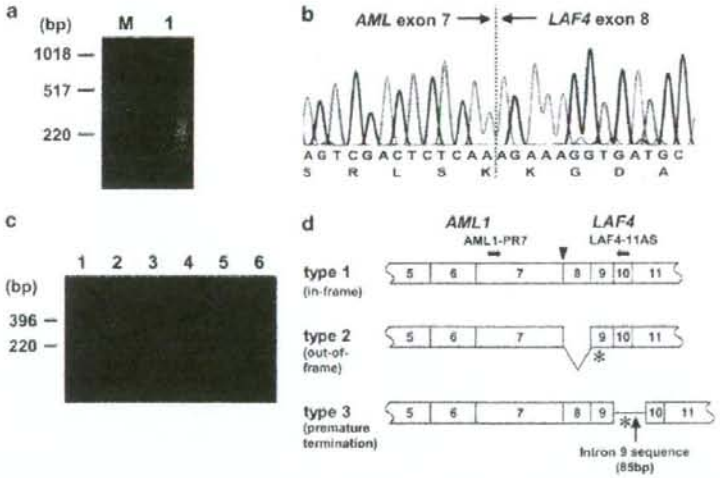

Figure 3 Identification of *AML1-LAF4* fusion transcript. (**a**) Bubble PCR products by nested PCR using AML1-5S and NVAMP1 for first PCR, and AML1-E6S and NVAMP2 for second PCR (lane 1). M, size marker. (**b**) Sequence analysis of *AML1-LAF4* fusion transcript. The single letter amino-acid sequences surrounding the fusion point are shown at the bottom of the figure. (**c**) Detection of *AML1-LAF4* fusion transcripts by reverse transcription-PCR. Primers were AML1-PR7 and LAF4-11AS (lanes 1 and 3), AML1-PR8 and LAF4-PR5 (lanes 2 and 4), and β-actin, respectively. Lanes 1, 3 and 5, patient's leukemic cells; lanes 2, 4 and 6, normal peripheral lymphocytes. (**d**) Three fusion transcripts of *AML1-LAF4* are schematically depicted. Gray/dotted boxes denote predicted *AML1* exons and white boxes represent predicted *LAF4* exons. Type 3 contains the *LAF4* intron 9 splicing donor site. AML1-PR7 and LAF4-11AS indicate the primers used for reverse transcription-PCR. Asterisk shows the termination codon.

approximately 11 kb *Bgl*II germline fragment on chromosome 21 (data not shown). To isolate the fusion point of chromosomes 2 and 21, we next performed bubble PCR on genomic DNA and detected nested PCR products using primers AML1-GNM8-2S and NVAMP2 (Figure 4a). Sequence analysis of the subcloned PCR product revealed the genomic junction of 5′-*AML1-LAF4*-3′ (Figures 4c and d), and the result

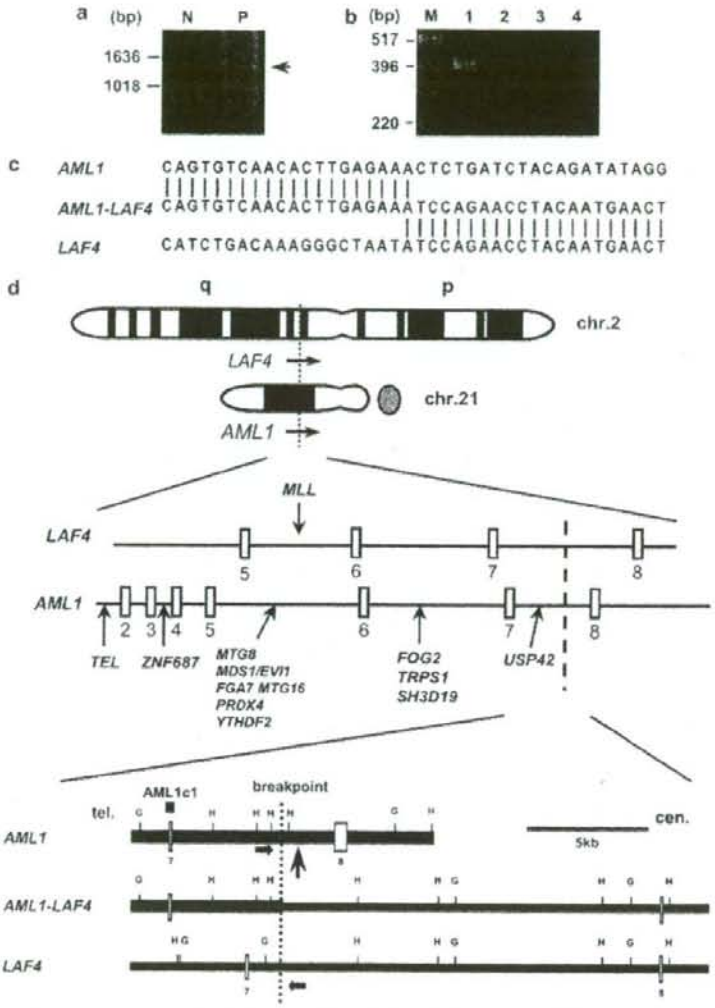

Figure 4 Cloning of the genomic junction of *AML1* and *LAF4*. (**a**) Bubble PCR for genomic DNA. N, normal human lymphocytes; P, patient's leukemic cells. (**b**) Detection of the genomic fusion point of *AML1-LAF4* by PCR. Primers were AML1-GNM8-4S and LAF4-GNM11-2AS (lanes 1 and 3), and LAF4-GNM11-2S and AML1-GNM8-2AS (lanes 2 and 4). Lanes 1 and 2, patient's leukemic cells; lanes 3 and 4, normal peripheral lymphocytes. M, size marker. (**c**) Sequences of breakpoints in the patient's leukemic cells. (**d**) Physical map of the breakpoint regions. Open vertical boxes represent defined exons in each gene. Horizontal arrows show the primers used. Restriction sites are indicated by capital letters: G, *Bgl*II; H, *Hind*III. AML1c1 indicates the position of the cDNA probes for Southern blot analysis. A vertical arrow shows *AML1-USP42* breakpoint.

was confirmed by PCR analysis using primers AML1-GNM8-4S and LAF4-GNM11-2AS (Figure 4b); however, no *5'-LAF4-AML1-3'* product was generated, suggesting interstitial deletion near genomic break points (Figure 4b). These sequences near the break points did not contain any lymphoid heptamer/nonamer sequences, *Alu* sequences or consensus topoisomerase II cleavage sites.

Discussion

In this study, we identified that *LAF4* was fused to *AML1* in pediatric T-ALL with t(2;21)(q11;q22). Other regions with chromosomal aberrations in this patient were not considered to be associated with recurrent cytogenetic changes involving T-ALL, except for the deletion of the short arm of chromosome 9. Spectral

karyotyping analysis detected del(9)(p13), and additional analysis of genome array (Human Mapping 50 K Hind Array, Affymetrix, Tokyo, Japan) revealed homozygous deletion of 4.5 Mb within the 9p21 region, including the *CDKN2A/p16/p14* locus (data not shown), which is frequently deleted in T-ALL (Ohnishi *et al.*, 1995).

Although the patient showed a complex chromosomal abnormality, t(2;21)(q11;q22) can form regular head-to-tail fusion transcripts of both *AML1* and *LAF4*, because the transcription direction of *AML1* and *LAF4* is telomere to centromere. Furthermore, fluorescence *in situ* hybridization analysis revealed two der(2)t(2;21)(q11.2;q22) creating *5′-AML1-LAF4-3′*, suggesting that *5′-AML1-LAF4-3′* is critical for leukemogenesis.

LAF4 was previously reported to be a fusion partner of *MLL* in pediatric B-precursor ALL with t(2;21)(q11;q23) (von Bergh *et al.*, 2002; Bruch *et al.*, 2003; Hiwatari *et al.*, 2003). *LAF4* is the first gene fused to both *AML1* and *MLL*, and both *AML1-LAF4* and *MLL-LAF4* contained the same domains of *LAF4* (Figure 5). During the preparation of this manuscript, we found another pediatric T-ALL patient with *AML1-LAF4* reported in the Meeting Abstract (Abe *et al.*, *Blood* (ASH Annual Meeting Abstracts) 2006; **108**: 4276), suggesting that t(2;21)(q11;q23) is a recurrent cytogenetic abnormality and that the *AML1-LAF4* fusion gene is associated with the T-ALL phenotype. Both putative fusion proteins of AML1-LAF4 observed in two patients contained the Runt domain of AML1, and the transactivation domain, nuclear localization sequence and C-terminal homology domain of LAF4, although the fused exon of *LAF4* differed in the two cases. Several studies have reported that the fusion partners of *MLL* fused with different genes such as *MLL-AF10* and *CALM-AF10*, *MLL-CBP* and *MOZ-CBP* or *MLL-p300* and *MOZ-p300* (Ida *et al.*, 1997; Taki *et al.*, 1997; Chaffanet *et al.*, 2000). Comparison of the structure and function between *AML1-LAF4* and *MLL-LAF4* will facilitate our understanding of the molecular mechanisms underlying *AML1*- and *MLL*-related leukemia.

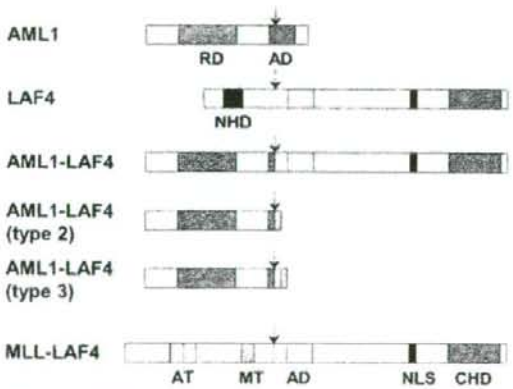

Figure 5 Schematic representation of putative AML1, LAF4 and AML1-LAF4 fusion proteins. Putative MLL-LAF4 fusion protein is also indicated for comparison. Arrows, break points or fusion points; AD, transactivation domain; AT, AT hooks; CHD, C-terminal homology domain; DNA, methyltransferase homology region; RD, RUNT domain; MT, DNA methyltransferase homology region; NLS, nuclear localization sequence.

The only *AML1* fusion partners in T-ALL are *LAF4* and *FGA7*. It is not known how *FGA7* is associated with T-ALL leukemogenesis, because *FGA7* does not show any significant sequence homology to any known protein motifs and/or domains (Mikhail *et al.*, 2004). Both patients with *AML1-LAF4* and *MLL-LAF4* fusions were diagnosed as having ALL, but they have different lymphoid lineages. *MLL-LAF4* is associated with B-lineage ALL; however, *AML1-LAF4* generates T-ALL. Our previous study showed that *LAF4* was expressed not only in B-lineage ALL but also in T-lineage ALL cell lines (Hiwatari *et al.*, 2003). *LAF4* showed strong sequence similarity to *AF4* (Ma and Staudt, 1996), which has a role in the differentiation of both B and T cells in mice (Isnard *et al.*, 2000). Furthermore, it was reported that *AML1* also plays an important role in T- and B-cell differentiation, because *AML1*-deficient bone marrow increased defective T- and B-lymphocyte development (Ichikawa *et al.*, 2004). These findings support that both *AML1* and *LAF4* are associated with T-ALL, respectively. Further functional analysis of the *AML1-LAF4* fusion gene will provide new insights into the leukemogenesis of *AML1*-related T-ALL. Recently, it has been reported that C-terminal truncated AML1-related fusion proteins play critical roles in leukemogenesis (Yan *et al.*, 2004, Agerstam *et al.*, 2007), suggesting that the two additional types of fusion transcripts observed in our patient (types 2 and 3 in Figures 3d and 5) have an additional function in leukemogenesis other than that of the entire AML1-LAF4 fusion protein.

In this study, we first applied the panhandle PCR method, which is usually used for cloning the fusion partners of *MLL* or *NUP98* (Megonigal *et al.*, 2000; Taketani *et al.*, 2002); however, no fusion transcripts could be obtained. Therefore, we searched for another method to clone the fusion transcripts and adapted the bubble PCR method for cDNA cloning. To date, bubble PCR has been performed for cloning unknown genomic fusion points but not fusion cDNAs (Zhang *et al.*, 1995). Using double-stranded cDNA, we could apply the bubble PCR method for cloning fusion cDNA with fewer nonspecific products. The bubble PCR primer can only prime DNA synthesis after a first-strand cDNA has been generated by an *AML1*-specific primer because of the bubble-tag with an internal non-complementary region (Zhang *et al.*, 1995). Although bubble PCR for genomic DNA generated one or two amplification products (Smith, 1992), bubble PCR for cDNA generated a complex set of amplification products that appeared as a smear by SYBR green staining, suggesting that a random hexamer generated various double-stranded cDNA containing the *AML1* sequence. This means that various fusion points can be estimated, even if after bubble oligo ligation was generated. Furthermore, bubble PCR for cDNA could amplify in both 5′–3′ and 3′–5′ directions of the gene or transcript, and easily

Table 1 Comparison between bubble PCR and panhandle PCR

Characteristics	*Bubble PCR*	*Panhandle PCR*
Available orientation of fusion transcript	5′-3′, 3′-5′	Only 5′-3′
AML1-specific random hexamer[a]	Not necessary	Necessary
Self-annealing	Not necessary	Necessary
Number of required polymerase reaction	2	4
Number of final products	Many (smear)	A few
Nonspecific product	Few	Few
Number of extra sequences other than targeted sequences in cloned product	50–60 bp	> 100 bp
Search for other targeted exons	Easy	Hard[b]

[a]30-mers *AML1*-specific oligonucleotide with random hexamer (AML1-N). [b]Necessary to use another *AML1*-specific random hexamer if the target exons are 5′ region of the initial target.

handle any exons fused to unknown partners for amplification. Once-ligated cDNAs are also available for cloning any genes, other than *AML1*, as the target. We demonstrated the efficiency and specificity of bubble PCR for cDNA (Table 1 and Supplementary Figure S2).

To date, a great number of fusion genes associated with chromosomal translocations have been cloned, although these fusion genes are found as a minor part of various malignancies. Recently, high frequencies of mutations in *NOTCH1* in T-ALL (James *et al.*, 2005), *NPM* in AML with normal karyotype (Weng *et al.*, 2004) and *JAK2* in myeloproliferative disorders (polycythemia vera, essential thrombocythemia and idiopathic myelofibrosis) (James *et al.*, 2005) have been reported, and these mutations are considered to be a good target for therapy. These genes were first identified as associated with chromosomal translocations in a small subset of specific phenotypes of hematologic malignancies (Ellisen *et al.*, 1991; Morris *et al.*, 1994; Lacronique *et al.*, 1997). These findings suggest that continuing attempts to identify genes associated with chromosomal translocations can be expected to provide further insights into the significance of various gene alterations in cancer and the development of novel-targeted therapies (Taki and Taniwaki, 2006). The bubble PCR method for cDNA will contribute to identifying numerous novel translocation partners more easily and further functional analysis of chimeric transcripts.

Materials and methods

Spectral karyotyping analysis
Spectral karyotyping analysis was performed with a Sky-Painting kit (Applied Spectral Imaging, Migdal Ha'Emek, Israel). Signal detection was performed according to the manufacturer's instructions.

Fluorescence in situ *hybridization analysis*
Fluorescence *in situ* hybridization analysis of the patient's leukemic cells using *AML1*-specific BAC clones (RP11-272A3, 3′ of *AML1* and RP11-994N6, 5′ of *AML1*) was carried out as described previously (Taniwaki *et al.*, 1994). Fusion of *AML1* and *LAF4* was analysed with the patient's leukemic cells using RP11-994N6 (5′ of *AML1*) and RP11-527J8 (3′ of *LAF4*).

Bubble PCR for cDNA
We modified the original bubble PCR method to apply for cDNA cloning (Figure 2; Supplementary Figure S2) (Smith, 1992; Zhang *et al.*, 1995).

Poly(A)$^+$ RNA was extracted from the patient's leukemic cells using a QuickPrep Micro mRNA Purification Kit (GE Healthcare, Buckinghamshire, UK). Two hundred nanograms of poly(A)$^+$ RNA was reverse transcribed to cDNA in a total volume of 33 μl with random hexanucleotide using the Ready-To-Go You-Prime First-Strand Beads (GE Healthcare). Double-stranded cDNAs were synthesized from 10 μl of single-stranded cDNA with a phosphorylated random hexanucleotide, blunt ended with T4 DNA polymerase, digested with *Rsa*I endonuclease and ligated with bubble oligo. *Rsa*I, a 4-bp blunt-ended cutter, was chosen to shorten the bubble oligo-ligated fragments, so that almost all bubble oligo-ligated fragments would be easy to clone by standard PCR reaction. This suggests that poor-quality samples are also suited to this method, although it is unsuitable for cloning long products.

The sequences of the primers used are listed in Supplementary Table S1 and their positions in the *AML1* gene are shown in Supplementary Figure S2. Nested PCR was performed using primers NVAMP-1 (bubble oligo) and AML1-5S (exon 5) for first round PCR, and NVAMP-2 (bubble oligo) and AML1-E6S (exon 6) for nested PCR. NVAMP1 and NVAMP2 can only anneal to the newly synthesized unique sequence of the bubble oligo by AML1-5S.

We used poly(A)$^+$ RNA in bubble PCR for cDNA with the expectation that this approach could amplify fewer transcripts; however, total RNA is also suitable for this method.

Bubble PCR for genomic DNA
Bubble PCR for genomic DNA was performed as described previously (Smith, 1992; Zhang *et al.*, 1995). Primers were as follows: NVAMP-1 and AML1-GNM8S for first round PCR, and NVAMP-2 and AML1-GNM8-2S for second round PCR (Supplementary Table S1).

Reverse transcription–PCR and genomic PCR analyses
Reverse transcription–PCR and genomic PCR analyses were performed as described previously. After 35 rounds of PCR (30 s at 94 °C, 30 s at 55 °C, 1 min at 72 °C), 5μl of PCR product were electrophoresed in a 3% agarose gel. Primers were as follows: AML1-PR7 and LAF4-11AS, and AML1-PR8 and LAF4-PR5 for reverse transcription-PCR; and AML1-GNM8-4S and LAF4-GNM11-2AS, and LAF4-GNM11-2S and AML1-GNM8-2AS for genomic PCR (Supplementary Table S1).

Nucleotide sequencing
Nucleotide sequences of PCR products and, if necessary, subcloned PCR products were analysed as described previously (Hiwatari *et al.*, 2003).

Southern blot analysis
High-molecular-weight DNA was extracted from the patient's leukemic cells by proteinase K digestion and phenol/chloroform extraction. DNA (10 μg) was digested with *Bgl*II, subjected to electrophoresis on 0.7% agarose gel and transferred to a nylon membrane. Blots were hybridized to probes that were labeled by the Dig-labeled PCR method according to the manufacturer's instructions (Roche Applied Science, Tokyo, Japan). Probes

were 112 bp *AML1* cDNA fragments (AML1c1, nucleotides 1233–1344; GenBank accession no. NM_001754).

Abbreviations

AML, acute myeloid leukemia; ALL, acute lymphoblastic leukemia.

Acknowledgements

We express our appreciation for the outstanding technical assistance of Kozue Sugimoto, Minako Goto and Kayoko Kurita. This work was supported by a grant-in-aid for Scientific Research (B) from the Ministry of Education, Culture, Sports, Science and Technology of Japan, and the Takeda Science Foundation.

References

Agerstam H, Lilljebjorn H, Lassen C, Swedin A, Richter J, Vandenberghe P *et al.* (2007). Fusion gene-mediated truncation of *RUNX1* as a potential mechanism underlying disease progression in the 8p11 myeloproliferative syndrome. *Genes Chromosomes Cancer* **46**: 635–643.

Asou N, Yanagida M, Huang L, Yamamoto M, Shigesada K, Mitsuya H *et al.* (2007). Concurrent transcriptional deregulation of AML1/RUNX1 and GATA factors by the *AML1-TRPS1* chimeric gene in t(8;21)(q24;q22) acute myeloid leukemia. *Blood* **109**: 4023–4027.

Bruch J, Wilda M, Teigler-Schlegel A, Harbott J, Borkhardt A, Metzler M. (2003). Occurrence of an *MLL/LAF4* fusion gene caused by the insertion ins(11;2)(q23;q11.2q11.2) in an infant with acute lymphoblastic leukemia. *Genes Chromosomes Cancer* **37**: 106–109.

Chaffanet M, Gressin L, Preudhomme C, Soenen-Cornu V, Birnbaum D, Pebusque MJ. (2000). *MOZ* is fused to *p300* in an acute monocytic leukemia with t(8;22). *Genes Chromosomes Cancer* **28**: 138–144.

Chan EM, Comer EM, Brown FC, Richkind KE, Holmes ML, Chong BH *et al.* (2005). *AML1-FOG2* fusion protein in myelodysplasia. *Blood* **105**: 4523–4526.

Ellisen LW, Bird J, West DC, Soreng AL, Reynolds TC, Smith SD *et al.* (1991). *TAN-1*, the human homolog of the Drosophila *Notch* gene, is broken by chromosomal translocations in T lymphoblastic neoplasms. *Cell* **66**: 649–661.

Erickson P, Gao J, Chang KS, Look T, Whisenant E, Raimondi S *et al.* (1992). Identification of breakpoints in t(8;21) acute myelogenous leukemia and isolation of a fusion transcript, AML1/ETO, with similarity to *Drosophila* segmentation gene, runt. *Blood* **80**: 1825–1831.

Gamou T, Kitamura E, Hosoda F, Shimizu K, Shinohara K, Hayashi Y *et al.* (1998). The partner gene of *AML1* in t(16;21) myeloid malignancies is a novel member of the *MTG8* (*ETO*) family. *Blood* **91**: 4028–4037.

Golub TR, Barker GF, Bohlander SK, Hiebert SW, Ward DC, Bray-Ward P *et al.* (1995). Fusion of the *TEL* gene on 12p13 to the *AML1* gene on 21q22 in acute lymphoblastic leukemia. *Proc Natl Acad Sci USA* **92**: 4917–4921.

Grimwade D, Walker H, Oliver F, Wheatley K, Harrison C, Harrison G *et al.* (1998). The importance of diagnostic cytogenetics on outcome in AML: analysis of 1,612 patients entered into the MRC AML 10 trial. The Medical Research Council Adult and Children's Leukaemia Working Parties. *Blood* **92**: 2322–2333.

Hayashi Y. (2000). The molecular genetics of recurring chromosome abnormalities in acute myeloid leukemia. *Semin Hematol* **37**: 368–380.

Hiwatari M, Taki T, Taketani T, Taniwaki M, Sugita K, Okuya M *et al.* (2003). Fusion of an *AF4*-related gene, *LAF4*, to *MLL* in childhood acute lymphoblastic leukemia with t(2;11)(q11;q23). *Oncogene* **22**: 2851–2855.

Ichikawa M, Asai T, Saito T, Seo S, Yamazaki I, Yamagata T *et al.* (2004). *AML-1* is required for megakaryocytic maturation and lymphocytic differentiation, but not for maintenance of hematopoietic stem cells in adult hematopoiesis. *Nat Med* **10**: 299–304.

Ida K, Kitabayashi I, Taki T, Taniwaki M, Noro K, Yamamoto M *et al.* (1997). Adenoviral E1A-associated protein p300 is involved in acute myeloid leukemia with t(11;22)(q23;q13). *Blood* **90**: 4699–4704.

Isnard P, Core N, Naquet P, Djabali M. (2000). Altered lymphoid development in mice deficient for the m*AF4* proto-oncogene. *Blood* **96**: 705–710.

James C, Ugo V, Le Couedic JP, Staerk J, Delhommeau F, Lacout C *et al.* (2005). A unique clonal *JAK2* mutation leading to constitutive signalling causes polycythaemia vera. *Nature* **434**: 1144–1148.

Kurokawa M, Hirai H. (2003). Role of AML1/Runx1 in the pathogenesis of hematological malignancies. *Cancer Sci* **94**: 841–846.

Lacronique V, Boureux A, Valle VD, Poirel H, Quang CT, Mauchauffe M *et al.* (1997). A TEL-JAK2 fusion protein with constitutive kinase activity in human leukemia. *Science* **278**: 1309–1312.

Ma C, Staudt LM. (1996). *LAF-4* encodes a lymphoid nuclear protein with transactivation potential that is homologous to *AF-4*, the gene fused to *MLL* in t(4;11) leukemias. *Blood* **87**: 734–745.

Megonigal MD, Rappaport EF, Wilson RB, Jones DH, Whitlock JA, Ortega JA *et al.* (2000). Panhandle PCR for cDNA: a rapid method for isolation of *MLL* fusion transcripts involving unknown partner genes. *Proc Natl Acad Sci USA* **97**: 9597–9602.

Mikhail FM, Coignet L, Hatem N, Mourad ZI, Farawela HM, El Kaffash DM *et al.* (2004). *FGA7*, is fused to *RUNX1/AML1* in a t(4;21)(q28;q22) in a patient with T-cell acute lymphoblastic leukemia. *Genes Chromosomes Cancer* **39**: 110–118.

Mitani K, Ogawa S, Tanaka T, Miyoshi H, Kurokawa M, Mano H *et al.* (1994). Generation of the *AML1-EVI-1* fusion gene in the t(3;21)(q26;q22) causes blastic crisis in chronic myelocytic leukemia. *EMBO J* **13**: 504–510.

Miyoshi H, Kozu T, Shimizu K, Enomoto K, Maseki N, Kaneko Y *et al.* (1993). The t(8;21) translocation in acute myeloid leukemia results in production of an *AML1-MTG8* fusion transcript. *EMBO J* **12**: 2715–2721.

Miyoshi H, Shimizu K, Kozu T, Maseki N, Kaneko Y, Ohki M. (1991). t(8;21) breakpoints on chromosome 21 in acute myeloid leukemia are clustered within a limited region of a single gene, *AML1*. *Proc Natl Acad Sci USA* **88**: 10431–10434.

Morris SW, Kirstein MN, Valentine MB, Dittmer KG, Shapiro DN, Saltman DL *et al.* (1994). Fusion of a kinase gene, *ALK*, to a nucleolar protein gene, *NPM*, in non-Hodgkin's lymphoma. *Science* **263**: 1281–1284.

Nguyen TT, Ma LN, Slovak ML, Bangs CD, Cherry AM, Arber DA. (2006). Identification of novel *Runx1* (*AML1*) translocation partner genes *SH3D19*, *YTHDf2*, and *ZNF687* in acute myeloid leukemia. *Genes Chromosomes Cancer* **45**: 918–932.

Ohnishi H, Kawamura M, Ida K, Sheng XM, Hanada R, Nobori T *et al.* (1995). Homozygous deletions of *p16/MTS1* gene are frequent but mutations are infrequent in childhood T-cell acute lymphoblastic leukemia. *Blood* **86**: 1269–1275.

Okuda T, Cai Z, Yang S, Lenny N, Lyu CJ, van Deursen JM *et al.* (1998). Expression of a knocked-in *AML1-ETO* leukemia gene inhibits the establishment of normal definitive hematopoiesis and directly generates dysplastic hematopoietic progenitors. *Blood* **91**: 3134–3143.

Paulsson K, Bekassy AN, Olofsson T, Mitelman F, Johansson B, Panagopoulos I. (2006). A novel and cytogenetically cryptic t(7;21)(p22;q22) in acute myeloid leukemia results in fusion of *RUNX1* with the ubiquitin-specific protease gene *USP42*. *Leukemia* **20**: 224–229.

Rowley JD. (1999). The role of chromosome translocations in leukemogenesis. *Semin Hematol* **36**: 59–72.

Smith DR. (1992). Ligation-mediated PCR of restriction fragments from large DNA molecules. *PCR Methods Appl* **2**: 21–27.